CHARACTERIZATION OF FLAME RETARDANTS ADDED ABS

CH'NG BOON SIN

A project report submitted in partial fulfilment of the requirements for the award of Bachelor of Engineering (Hons.) Chemical Engineering

Faculty of Engineering and Science
Universiti Tunku Abdul Rahman

April 2015

DECLARATION

I hereby declare that this project report is based on my original work except for citations and quotations which have been duly acknowledged. I also declare that it has not been previously and concurrently submitted for any other degree or award at UTAR or other institutions.

Signature : _____

Name : _____

ID No. : _____

Date : _____

APPROVAL FOR SUBMISSION

I certify that this project report entitled **"CHARACTERIZATION OF FLAME RETARDANTS ADDED ABS"** was prepared by **CH'NG BOON SIN** has met the required standard for submission in partial fulfilment of the requirements for the award of Bachelor of Engineering (Hons.) Chemical Engineering at Universiti Tunku Abdul Rahman.

Approved by,

Signature : _____

Supervisor : _____

Date : _____

Specially dedicated to
my beloved parents

ACKNOWLEDGEMENTS

I would like to thank everyone who had contributed to the successful completion of this project. I would like to express my gratitude to my research supervisor, Dr. Bee Soo Tueen for her invaluable advice, guidance and her enormous patience throughout the development of the research even though she was pregnant or during her maternity leave.

In addition, I would also like to express my gratitude to my friends who had helped and given me encouragement to complete this project. Without their cooperation, I would not able to solve the problems which I encountered during my research. Last but not least, I would like to say I had learnt a lot regarding polymer research and met new friends throughout the project. Last but not least, I would like to to express my appreciation to Malaysia Nuclear Agency, Bangi, Selangor for allowing me to use their equipments throughout my project. Without their kindliness, I would not able to conduct my research smoothly.

CHARACTERIZATION OF FLAME RETARDANTS ADDED ABS

ABSTRACT

Effect of zinc borate (ZB) and electron beam irradiation on aluminium trihydrate (ATH) and magnesium hydroxide (MOH) added acrylonitrile-butadiene-styrene (ABS) were investigated. The ZB was used to improve the flammability of ATH-ABS and MOH-ABS composites. The flame retardant samples were crosslinked using electron beam irradiation at dosage up to 250 kGy. The effect of ZB addition and electron beam irradiation was revealed by limiting oxygen index test (LOI). It was observed in limiting oxygen index (LOI) was improved 2 to 6 LOI% due to the synergistic benefits of metal hydroxide and ZB. Furthermore, the irradiated samples exhibited a slightly enhancement on flammability by 2 ~ 4 LOI% as compared to un-irradiated samples. Although the flammability of the composites was improved with the addition of ZB to ATH-ABS and MOH-ABS composites, its mechanical properties of the composites could be affected and then tensile test was carried out. The mechanical properties of the composites had slightly decreased as the loading level of ZB increased. Furthermore, the surface morphology of un-irradiated ZB added ATH-ABS composites showed ATH had a poor interfacial adhesion with ABS matrix whereas the surface morphology of MOH-ABS composites showed the presence of plenty bubble voids across the composites surface. On the other hand, the increasing irradiated dosage was significantly affected the crosslinking density and mechanical properties of the flame retardant samples. The irradiation dosage above 100 kGy was found to cause chain scission within ABS matrix. As the irradiation dosages continued to increase further, the crosslinking effect was then found to be greater than chain scission effect, subsequently improving the mechanical properties of flame retardant samples. Generally, this study has demonstrated that addition of ZB and electron beam irradiation to ATH-ABS and MOH-ABS composites have resulted better flammability but slightly decrement in mechanical properties.

TABLE OF CONTENTS

LIST OF TABLES

LIST OF FIGURES

LIST OF SYMBOLS / ABBREVIATIONS

σ	stress, MPa
F	deformation force, N
A	cross-section area of test marks before test, m^2
ε	strain, %
ΔL	change in gage length, mm
L_o	initial gage length, mm
L	gage length at break, mm
E	Young Modulus, MPa
W_A	weight of remaining sample (gel) after treatment by solvent, g
W_B	weight of initial sample (sol + gel)
LOI %	limiting oxygen index, %

ABS	Acrylonitrile-butadiene-styrene
ATH	Aluminium Trihydrate
MOH	Magnesium Hydroxide
ZB	Zinc Borate
SEM	Scanning Electron Microscopy
TEM	Transmission Electron Microscopy
LOI	Limiting Oxygen Index

CHAPTER 1

INTRODUCTION

1.1 Background

Fire retardant polymers are the polymers which have blended with fire retardants additive to prevent polymers to be easily burnt by fire and restrict the spreading of fire. Fire retardant polymers have been manufactured to become most of the goods use in the daily life; for example furniture, electronic, textiles, construction material and others. These fire retardant polymers have the flammability standards which meets the uses in different fields.

Acrylonitrile-butadiene-styrene (ABS) is terpolymer of thermoplastic as ABS are made up of acrylonitrile, butadiene and styrene monomers. ABS is widely used for tough products such as automotive parts, pipes, toys, containers, electronic devices, kitchen appliance and other consumer products. This terpolymer is famous with their ability to withstand high impact and mechanical strength. ABS is also widely applied as flame resistance field by blending fire retardant fillers with ABS.

The present of fire will bring out the concern of flame, smoke and toxic fume. Thus, flame retardants added ABS resin is commercialised for the safety of commercial user. There are different kinds of flame retardant fillers available in the market. In this study, three non-halogen flame retardant fillers which are alumina trihydroxide (ATH), magnesium hydroxide and zinc borate, have been selected to blend with ABS.

ATH and magnesium hydroxide fillers have the ability to decompose endothermically when encountering fires. Nevertheless, magnesium hydroxide has a higher decomposition temperature than ATH which able to absorb heat than ATH. When ATH and magnesium hydroxide reach their decomposition temperature, dehydration occurs. The water molecule released by ATH and magnesium hydroxide will reduce the temperature of heated ABS and prevent spreading of fires. Furthermore, ATH also acts as smoke suppressant. Zinc borate has a different flame retardant mechanism compare to ATH and magnesium hydroxide. Zinc borate promotes formation of char when heated. The char acts a barrier to prevent the penetration of oxygen into the polymer. Moreover, zinc borate is able to inhibit the formation of smoke and afterglow (Harwick Standard, 2008). The amount of flame retardant fillers blended with ABS will produce different level to withstand flame. The higher the flame retardants fillers added, the higher its flame resistance.

Though, the original mechanical properties of ABS will be affected after addition of fillers. Thus, crosslinking is used to enhance the mechanical and thermal properties of flame retarded ABS. Radiation process is one of the methods to apply crosslinking to the polymer. Radiation processing was familiarised more than half a century. This processing has been commercially applied to modify plastic and rubber products, and sterilize medical devices and consumer items. The developing applications are even used to pasteurizing and preserving foods, and reducing environmental pollution (Cleland, 2006). Electron beam irradiation crosslinking method is chosen as this method can improve the mechanical properties of matrix effectively. Furthermore, electron beam irradiation is more environmental friendly compare to other methods (Machi, 1996). Different irradiation dosage will produce different mechanical properties of matrix.

1.2 Problem Statements

Addition of flame retardants into ABS provides the flame retardant properties to the matrix however it would also detriment ABS original mechanical properties. Different blends of flame retardants with ABS would give different mechanical properties.

Furthermore, crosslinking of electron beam method was also used to improve the polymer flammability and mechanical properties. The problems were identified as below:

1. What is the effect of increasing zinc borate loading level on the mechanical, physical, flame retardancy and thermal properties of alumina trihydrate / zinc borate hybrid fillers added ABS composites?

2. What is the effect of increasing the loading level of zinc borate on the mechanical, physical, flame retardancy and thermal properties of magnesium hydroxide / zinc borate hybrid fillers added ABS composites?

3. What is the effect of increasing electron beam irradiation dosages on the mechanical, physical, flame retardancy and thermal properties of alumina trihydrate / zinc borate hybrid fillers added ABS composites and magnesium hydroxide / zinc borate hybrid fillers added ABS composites?

1.3 Aims and Objectives

The main objective of this study was to investigate the effect of increasing loading level of zinc borate and effect of irradiation dosage on the thermal and physico-mechanical properties of alumina trihydrate/ zinc borate added ABS composites and magnesium hydroxide/ zinc borate added ABS composites. In order to achieve the main objective of this study, the following sub-objectives were identified:

1. To investigate the effect of increasing zinc borate loading level on the mechanical, physical, flame retardancy and thermal properties of alumina trihydrate / zinc borate hybrid fillers added ABS composites.

2. To study the effect of increasing loading level of zinc borate on the mechanical, physical, flame retardancy and thermal properties of magnesium hydroxide / zinc borate hybrid fillers added ABS composites.

3. To examine the effect of increasing electron beam irradiation dosages on the mechanical, physical, flame retardancy and thermal properties of alumina trihydrate / zinc borate hybrid fillers added ABS composites and magnesium hydroxide / zinc borate fillers added ABS composites.

1.4 Scopes

In order to achieve the objectives, the following scopes are listed as below:

1. Preparation of ABS and flame retardants blend samples

   Blending of ABS resins with aluminium trihydrate, magnesium hydroxide and zinc borate was compounded using Barbender mixer operated at 180 ℃ and 50 rpm mixing speed for 12 minutes. The compound samples were then compression moulded into 1 mm thickness sheet at the heating temperature of 155℃. The compression moulded samples were then irradiated at the room temperature by using an electron beam accelerator.

2. Characterisation tests

   a) Tensile test

      Tensile test was conducted in according to ASTM D1822 by Instron Universal Testing Machine.

   b) Scanning electron microscopy analysis (SEM)

      The morphologies of the fracture surface for all samples from tensile test could be observed and studied by using a JEOL model JSM-6301F scanning electron microscope (SEM).

c) Limiting oxygen index test (LOI)

Limiting oxygen index test was conducted according to ASTM D2863 by using limiting oxygen index tester of Rheometer Scientific, United Kingdom.

d) Gel content test

The gel content level of flame retardants added ABS samples were measured in accordance to ASTM D2765.

CHAPTER 2

LITERATURE REVIEW

2.1 Acrylonitrile-Butadiene-Styrene (ABS)

The figure and table below show the molecular structure and properties of this terpolymer.

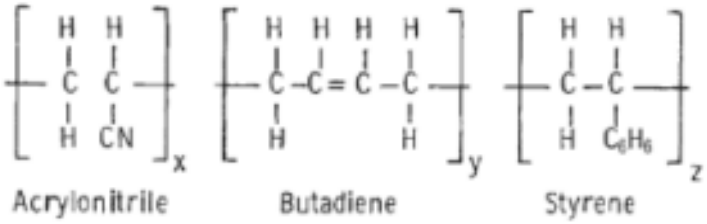

Figure 2.1: Molecular structure of acrylonitrile-butadiene-styrene (Harper and Petrie, 2003)

Table 2.1: Properties of General Purpose ABS (Harper and Petrie, 2003)

Property	General Purpose ABS
Specific Gravity	1.16 – 1.21
Tensile Strength, psi	3300 – 8000
Flexural Strength, psi	6200 – 14 000
Elongation, %	1.5 – 80
Izod Impact, ft·lb/in	1.4 – 12
Dielectric Strength, volts/mil	350 - 500

ABS occupies a major portion in thermoplastic market. This is because ABS has high strength and excellent resistance to impact due to the presence of rubbery butadiene. ABS plastic also has good resistance to acids and bases. It is recyclable and dimensional stable. This high impact ABS marks the boundary in price and performance between commodity and engineering thermoplastics (Fried, 2009). The moderate price and high impact properties of ABS made it famous in various application including automobile parts, piping, consumer products, telecommunications and others. The process melt temperature for ABS is in the range or 200 to 250 ºC (Dolbey, 1997). However, the low thermal conductivity of ABS causes some difficulty during moulding process by limiting ABS wall thickness. Moreover, ABS has weak weather and solvent resistance. When burning, it will generate large amount of smoke. ABS also not work well when exposed to ultra-violet rays. These disadvantageous limit the application of ABS. However, some of the weak performances on specific aspects can be improved by adding fillers or cross-linking.

2.2 Metal Hydroxides

In industry, there are two common metal hydroxides that used as flame retardants which are aluminium trihydrate (ATH) and magnesium hydroxide (MOH). Both inorganic hydroxides has the same flame retardancy mechanism which absorbs heat to decompose and release water. The heat provided by the flame is thus removed by the endothermic decomposition and cools down the flame. This phenomenon is named as "heat sink" (Xanthos, 2010). Xanthos also mentions that the flame retardancy mechanisms of these metal hydroxides can occur at condensed phase and gas phase.

There are three types of condensed phase processes. Firstly, flame retardants speed up the decomposition of polymer and thus cause the polymer to flow; hence lowering the impact from flame. Secondly, after burning, a layer of carbon will form on the surface of polymer and this process is called charring. This is because flame

retardant undergoes dehydration and leaves a flame impermeable layer. Thirdly, dehydration of flame retardant is an endothermic reaction and absorbs the heat from the flame. On the other hand, the gas phase flame retardancy mechanisms is normally depend on the combustion on flame retardant. During combustion process, flame retardants will form a free radical species. This free radical species will slow down the exothermic process that occur in the gas phase and results in cooling of the system and reduction in the supply of flammable gases (Xanthos, 2010).

When heating, metal hydroxides will absorbs heat and decompose. This endothermic decomposition cause the metal hydroxides to release its chemically bonded water molecule in gas phase; leaving the solid metal oxide as char residue. Through this decomposition, the heat energy of flaming zone is removed. Consequently, the leftover metal oxide of decomposition is then acting as a barrier to prevent the fire from reaching the inner side of the plastics. Moreover, this barrier also can inhibit the releasing of smoke. On the other hand, the release of water vapour into the atmosphere of burning zone can affect the critical fuel/oxygen ration. This mechanism prevent the ignition to occur (Xanthos, 2010).

The properties of aluminium hydroxide (ATH) and magnesium hydroxide (MOH) are presented by Table 2.2 at below.

Table 2.2: Properties of ATH and MOH (Walter & Wajer, n.d.; *"Alumina Trihydrate (ATH) & Magnesium Hydroxide (MDH)"*, n.d.)

Property	**ATH**	**MOH**
Bound Water, %	34.6	31.0
Specific Gravity	2.42	2.36
Mohs Hardness	2.5 – 3.5	2.0 – 3.0
Refractive Index	1.57	1.56 – 1.58
Colour	White	White
Physical Form	Powder	Powder
pH value	9 – 10	10 - 11
Initial Decomposition Temperature	220 ºC / 428 ºF	330 ºC / 626 ºF
Enthalpy of Decomposition, cal/g	280	328

Figure 2.2 shows the comparison of thermal degradation on aluminium hydroxide and magnesium hydroxide at different temperature. From the figure, magnesium hydroxide can withstand higher thermal degradation than aluminium hydroxide.

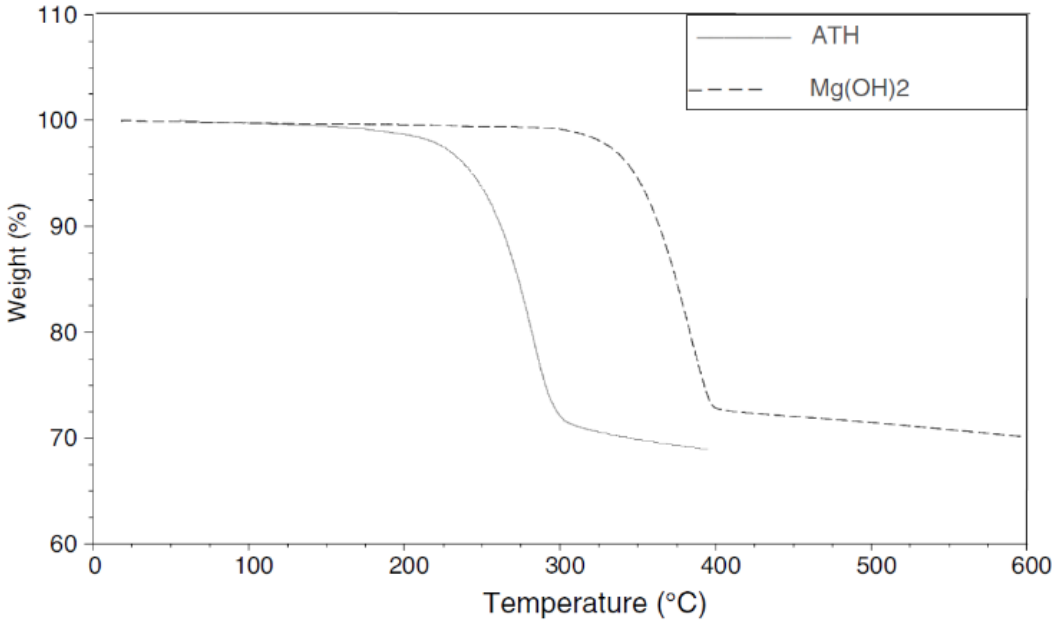

Figure 2.2: Thermal Degradation of ATH and MOH (Xanthos, 2010).

2.2.1 Aluminium Trihydroxide (ATH)

Aluminium trihydroxide is a white inorganic flame retardant fillers which functions at low temperature of burning. According to Table 3.2, the low refractive index makes the ATH contribute to low colouring properties. If there is about 50 % of ATH present in the mixture, the colour of the compound will be translucent. Furthermore, ATH has a relatively low initial decomposition temperature compare to other common flame retardant fillers. Its 220 ºC decomposition temperature limits the plastic processing temperature below its decomposition temperature. Nevertheless, this cheap metal

hydroxide makes it become the world biggest volume flame retardant used in plastic application such as automotive, construction, polymer casting, electrical or electronic devices, wire and cable. Contrarily, its performance on flame retardancy purpose is weak among those flame retardants. However, its weakness can be covered by blending with another high performance of flame retardants such as zinc borate, antimony or halogen type fillers.

This halogen-free base flame retardant decompose endothermically when heated. The chemical equation of decomposition of ATH (Xanthos, 2010):

$$2Al(OH)_3\,(s) \longrightarrow Al_2O_3\,(s) + 3H_2O\,(g) \qquad \Delta H = -298\ kJ/mole \qquad (2.1)$$

When heating upon the decomposition temperature of ATH, the solid state ATH will decompose endothermically and releasing solid aluminium oxide and water vapour (34.46 wt %). The heat capacity of $Al_2O_3{\cdot}3H_2O$ is 186.1 J/K·mol (Xanthos, 2010). Water vapour that released during the decomposition will dilute concentration of oxygen and flammable gases in the atmosphere directly surrounding of heated area (*"New ATH developments drive flame retardant cable compounding"*, 2002). The char (Al_2O_3) on the surface of burnt polymer has an excellent insulating behaviour that keep the inner plastic away from fire and prevent the propagation of fire into the deeper side of polymer. Additionally, this protective barrier will also inhibit the formation of smoke. High loading levels (more than 60 wt%) of ATH in the blends will give outstanding resistance to fire even contacting with red-hot metal (Xanthos, 2010).

2.2.2 Magnesium Hydroxide (MOH)

Although ATH acts as effective flame retardant and smoke suppressant for many polymer application, but its low processing temperature makes it cannot apply in thermoplastic, engineering thermoplastic, thermoset processing (Xanthos, 2010). Therefore, at high processing temperature, MOH will be preferred because MOH can perform better flame retardancy than ATH. The application of MOH is also almost

same as ATH application, for example, wire and cable, piping, electrical components, appliance houses, construction and others.

MgOH occurs as white powder at room temperature. The flame retardancy mechanism of MOH has the same manner as ATH. Just the big difference on the MOH endothermic dehydration occurs at 328 ºC. The liberation of MOH is shown at the chemical equation at below.

$$Mg(OH)_2\ (s) \longrightarrow MgO\ (s) + H_2O\ (g) \qquad \Delta H = -200\ kJ/mole \qquad (2.2)$$

From Table 2.2 of pH property, MOH is more alkaline than ATH; hence formation of a more alkaline MgO compare to Al_2O_3. This will reduce the chance of acidic, corrosive gases exiting the plastic when burning (Walter & Wajer, n.d.). Besides that, heat capacity of $MgO{\cdot}H_2O$ is just 77 J/K·mol and lower than the heat capacity of $Al_2O_3{\cdot}3H_2O$. Same as ATH, MOH also used in high loading level, usually in the range of 40 – 65 wt% (Xanthos, 2010).

2.3 Zinc Borate

Zinc borate is the most common borates that used as flame retardant fillers for polymer. The chemical formula of this fine zinc borate powder is $(ZnO)_x(B_2O_3)_y(H_2O)_z$ (Xanthos, 2010). Generally, the water content in zinc borate is between 1 to 26 % and the common zinc borate used in industry is $2ZnO{\cdot}3B_2O_3{\cdot}3.5H_2O$ (Katz and Milewski, 1987). Table below show the physical and chemical properties of zinc borate.

Table 2.3: Physical and chemical properties of zinc borate (Katz and Milewski, 1987)

Physical and Chemical Properties	Zinc Borate
Formula Weight	434
Colour	White
Refractive Index	1.58
Crystal Density, g/cm^3	2.8
Solubility	Virtually insoluble in water below 100 ºF; sparingly soluble at higher temperatures; can be hydrolysed with acids and bases

Zinc borate can be used as fire retardant in paint coating, manufacturing of PVC, polyesters, halogenated polyesters, polypropylene and others. Katz and Mileski (1987) have recommended that use of zinc borate with ABS resins. Zinc borate can be added into either halogen-containing polymer or halogen-free polymer. Halogen-containing polymer refers to zinc borate can be added into the polymer with antimony oxide. Besides that, zinc borate also can mix with ATH, MOH and phosphorus type flame retardant (Xanthos, 2010).

Through studies, zinc borate has the ability to replace the role of antimony oxide as flame retardant fillers in polymer. The reason is antimony oxide only function in vapour phase whereas zinc borate can function in condensed phase through pyrolysis and oxidation. When zinc borate encountering flame, it will stimulate the high molecular weight to form cellular char which acts as good insulator to protect underlying polymer and reduce the smoke emission.

There are different operating modes of flame retardant action complied by zinc borate. One of the famous manufacturers is U.S. Borax. First mode of zinc borate is presented by Borax's FIREBRAKE ZB. At temperature 290 – 450 ºC, FIREBRAKE ZB absorbs 503 J/g of heat to dehydrate and release about 13.5 % water (Horrocks and Price, 2001). The water discharge by the thermal degradation will cause the char to

blow and become a foam. The zinc and boron will form the char preventing the propagation of fire. Besides that, the water vapour will also dilute the fuel to make it more difficult to ignite or continue to burn. Next, there is another more stable zinc borate, FIREBRAKE 415, can sustain higher temperature compare to FIREBRAKE ZB. It starts to decompose at 415 ºC and best to apply in high processing temperature of thermoplastic.

The study from Chen and Shen (2005) shows that there is an improved flame retardancy mechanism when metal hydroxides used with zinc borate. Although high loading of metal hydroxide (typically 50 – 60 %) increase the properties to resist the fire and suppress the smoke, but it also cause some decreasing on mechanical properties of the polymer. Thus, boron-based flame retardant can be used with metal hydroxide to perform synergistically on fire performance and rheological. When metal hydroxides decompose thermally with zinc borate, they will form a porous and hard char which can perform as inhibitor layer for heat and mass transfer. In the report published by Chen and Shen, the best loading level of zinc borate to work effectively with magnesium hydroxide is in the range of 5 – 10 wt% of the compound. Furthermore, they also conclude that the higher the MOH:ZB ration used, the slower the heat release from the compound. In addition, they also found out that if using MOH-zinc borate system as flame retardant system, the processing of the compound will be easier due to formation of a more desirable particle packing between MOH and zinc borate parties when being inter-dispersed in the polymer. This benefit also the combination of metal hydroxide and zinc borate to apply in high molecular weight polymer which can reduce the decreasing of mechanical property of the compound. The fire performance of MOH/zinc borate system is almost same with the fire performance by ATH/zinc borate system but degree of heat reduction of ATH/zinc borate is lower than MOH/zinc borate combination. This is because zinc borate forms a better heat and mass protective barrier with MgO than Al_2O_3. Furthermore, from the studies by Chen and Shen, MOH works better with FIREBRAKE ZB instead of FIREBRAKE 415. However, there is an exothermic structure change may happen at elevated temperature when dehydrated FIREBRAZE ZB reacts with MgO (formed in dehydration of MOH) to generate magnesium orthoborate, $3MgO{\cdot}B_2O_3$ and zinc oxide, ZnO whereas FIREBRAKE 415 does not have such crystallinity changes.

2.4 Cross Linking Process

When ABS blends with ATH/zinc borate hybrid filler or MOH/zinc borate hybrid filler, there will be expected result on reduction of original ABS physical/mechanical properties. Therefore, crosslinking method is introduced to improve the mechanical properties of the blends. From the definition published in Polymer Science Dictionary (Alger, 1997), through crosslinking between atoms or groups, a cross-linked polymer is formed when the linear polymer chains are connected to each other through chemical bonds; forming 3-dimensional network. The crosslinking of polymer through this chemical bonds can be performed as intra- and intermolecular as shown in Figure 2.3.

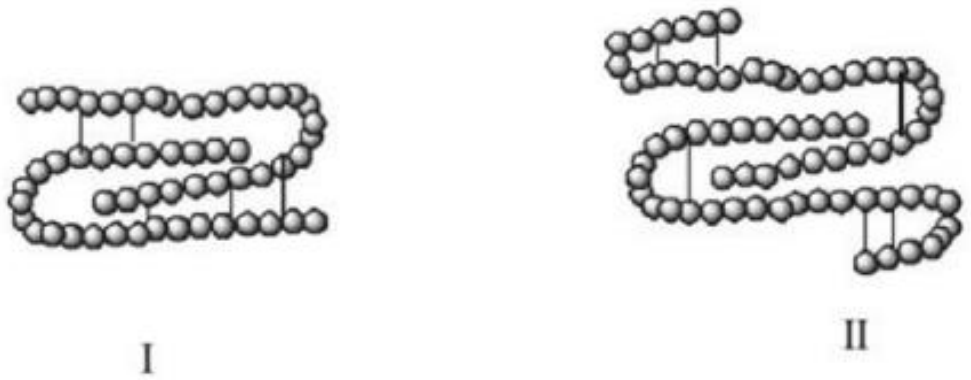

Figure 2.3: Schematic diagram for crosslinking as (I) intramolecular and (II) intermolecular (Bhattacharya, Rawlins and Ray, 2009)

There are many crosslinking method used in industry application. In general, crosslinking process can be performed by either radiation method or chemical cross linking method. The cross-linked polymer will have enhanced properties than uncross-linked polymer:

- Higher tensile strength
- Better abrasion resistance
- Good crush resistance

- Resist to solder iron
- Better performance during overloading
- Good stress cracking resistance
- Increase crystallinity
- Improved flame resistance
- Low flexibility
- Better performance on elevated temperature
  (*Polymer Crosslinking*, n.d.)

2.4.1 Radiation Crosslinking Method

Radiation cross inking is carried out by subjecting the polymer to high energy. Generally, the radiation sources that used in industry can be obtained via gamma rays from isotopes, electron beam from electron accelerators and X-rays produced by accelerators. Gamma-rays are produced through decaying of radioactive element such as cobalt-60 and cesium-137. This energy contained in this radiation is in between the energy of ultraviolet and X-rays (Makuuchi and Cheng, 2012). For electron beaming, the electron accelerator will generate high energy electrons to induce the crosslinking effect within polymer. Different energy levels of electron accelerator is used for different application. Table 2.4 describes the application of different energy levels of electron accelerator. Although electron beam has high energy and can supply in high dosage, but it cannot used to irradiate the thick polymer due to its penetration limit. Thus, X-rays is used instead of electron beaming for thick polymer crosslinking process but the electron accelerator is not effective on conversion of electron beam to X-ray. Table 2.5 compares the irradiation technologies mentioned at this section.

Table 2.4: Application of electron accelerators at different energy levels (Makuuchi and Cheng, 2012)

Type of Energy	Rating Range (MeV)	Features	Main Applications
Low	< 0.3	- Low penetration -Easy Shielding -Small machine size	-Surface coating -Thin film crosslinking
Medium	0.3 – 5	-Medium penetration	-Crosslinking of plastic parts
High	> 5	-High penetration -Heavy shielding	-Sterilization -Crosslinking -Degradation of polymers

Table 2.5: Comparison of irradiation technologies of gamma-rays, electron beam and X-ray (Makuuchi and Cheng, 2012)

Characteristic	Gamma-Ray	Electron Beam	X-Ray
Penetration	Strong, exponential attenuation	Limited range	Strong, exponential attenuation
Power	Low	High	Low
Operating Cost	Higher	Lower	Low
Dose Rate	Low	High	Low
Power Source	Radioactive isotope	Electricity	Electricity
Equipment	Easy to operate and maintain	Complicated to operate and maintain	Complicated to operate and maintain
Shielding	Continuous radiation requires more shielding	Can be turned on and off, less demanding in shielding	Can be turned on and off, less demanding in shielding
Source Attenuation	Continuous attenuation requires regular addition of source	No attenuation	No attenuation

By comparing these three irradiation technologies in Table 2.5, it is very obvious that electron beaming process is more preferable and because it can generate high power with low operating cost. Besides that, only electricity is needed to generate radiation instead of consumption on radioisotopes.

2.4.2 Chemical Crosslinking Method

Two common chemicals used as crosslinking agent are peroxides and silanes. These two chemicals reagents will chemically modify the polymer chain such as PVC, HDPE and others. In the work of Tendero, Jiménez, Greco and Maffezzoli, chemical crosslinking process is thermally activated during extrusion or mixing. However, requirement of heat is required when using peroxides chemical crosslinking. For silane crosslinking technique, the processing step requires the addition of water either in liquid or steam phase (*"Radiation vs. Chemical Crosslinking for Polymer Parts"*, 2005).

The common characteristic between these two types chemical crosslinking is addition of reactive groups into the polymer chains. Thus, the crosslinking is mainly depend on the reactivity of the reactive groups and the rate of reaction to create networks between polymer chains. These factors can affect the rate of cross linking:

a) Processing temperature
b) Presence of radiation
c) External reactants (such as O_2, H_2O, etc.)
d) Processing step

(Tillet, Boutevin and Ameduri, 2011)

In the peroxide crosslinking process, peroxides decompose thermally and produce free radicals. These free radicals contain high energy and then abstract hydrogen atoms from polymer chains to form macro-radicals. Macro-radicals will then form crosslink network by connecting to each other. The silane moisture-cure technology has the same working mechanism with peroxide crosslinking technology

by absorption of the silane onto polymer backbone and creating connection between polymer chains. However, the polymers are linked through siloxane bond in silane crosslinking process instead of carbon to carbon bond in peroxides treatment. This Si-O-Si are less rigid than C-C bonds. This polymers cured by silane will be more flexible than peroxide cured polymers (Smits and Materne, 2005).

2.4.3 Comparison between Radiation and Chemical Crosslinking

There is advantageous and disadvantageous between radiation and chemical crosslinking. Bhattacharya (2000) states that radiation cross linking has more advantages than chemical crosslinking. This is because radiation does not use another chemical to lower the activation energy of the reaction as it does not concern on the activation energy of the reaction. Besides that, the concentration of initiators will affect the chemical initiation whereas the radiation initiation is depend on the dosage of the radiation which is more easily to be controlled. In addition, the chemical that added for crosslinking may bring some issue on the contamination on the polymer which may affect the testing for research purpose. As mention in Section 2.4.2 at above, temperature is one of the condition to perform crosslinking using chemical. However, radiation-based crosslinking process is independent on temperature condition. On the other hand, radiation crosslinking requires a high technology electron accelerator and the running cost is more expensive than using the chemical-based crosslinking process. Comparing in terms of efficiencies, radiation techniques is more efficient than chemical technique.

In a nutshell, electron beaming can be said the most convenient technique. This is because electron beaming is more environmental friendly (Machi 1996).

2.5 Tensile Test

ABS is rubber strengthened thermoplastics which famous on their high impact properties for industrial application. Adding fillers into the virgin ABS will manipulate its original mechanical properties. The fillers may either improve or worsen the mechanical properties of new blends depend on the behaviour of filler in the polymer matrix. There are several methods to determine the mechanical performance of polymer. The methods are classified as:

a) Static (tensile and shear)
b) Transient (creep and stress relaxation)
c) Impact
d) Cyclic

(Fried, 2009)

Hence, the static tensile test is chosen to determine the mechanical properties of blended polymers. Tensile stress and strain are important aspects in static tensile test. Stress, σ and strain, ε are expressed respectively as formulas below.

$$\sigma = \frac{F}{A_o} \tag{2.5}$$

Where F is deformation force;

A_o is cross-sectional area of test marks before testing.

$$\varepsilon = \frac{\Delta L}{L_o} \tag{2.6}$$

Where ΔL is change in gage length $(L - L_o)$;

L_o is initial gage length;

L is gage length at break.

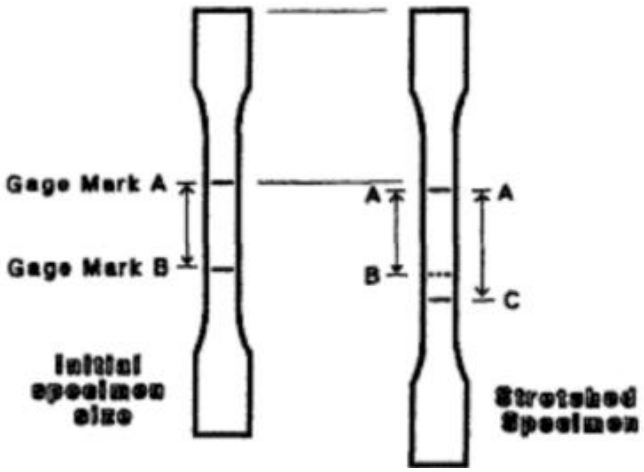

Figure 2.4: Illustration on the stretching the tensile dog sample (Driscoll, 1998)

In tensile test, the mechanical properties of the testing sample can be described and compared using the graph plotted as stress versus strain. Hooke's law is used to relate the stress and strain. As shown in Equation 2.7, the tensile modulus or Young's Modulus is the gradient of linear part of the curve. Hooke's law:

$$\sigma = E\varepsilon \tag{2.7}$$

Where E is Young's Modulus.

From the result of tensile test, we need to interpret by relating the loading of flame retardants to the tensile strength and elongation at break. In short, two types of graphs are constructed as tensile strength versus loading of flame retardants and elongation at break versus loading of flame retardants.

The loading of flame retardants will affect the mechanical properties of polymer blends. In the work of Zhang, et al. (2005), when ATH is added into EVA, there is an increase on the Young's modulus but decrease on tensile strength and elongation at break. Adding ATH into the polymer will decrease the mechanical properties of polymer. Similar result can apply to the addition of MOH to the LDPE and cross-linked polyethylene (XLPE) (Liu, 2014). Liu has compared the pure polyethylene (as LDPE and XLPE) with the MOH added polyethylene. From the result,

the presence of MOH improve the tensile modulus but cause reduction on the tensile strength and elongation. The addition of zinc borate to polymer such as wood flour-polyvinyl chloride (WF-PVC) will give increment to polymer's tensile modulus and flexural modulus. However, it also cause decrement to the tensile strength and flexural strength of WF-PVC (Fang, et al., 2013).

Furthermore, irradiation dosage may affect the mechanical properties of blended polymer. The study (Bee, et al., 2013) regarding how loading of MMT and irradiation dosage affect the mechanical properties of ATH added LDPE-EVA blends shows the tensile strength of the polymer blends has improved if the sample (low loading level of MMT) is exposed to dosage below 150 kGy. The improvement is due to crosslinking effect from electron beaming. However, a higher irradiation at 250 kGy gives different result as it may depend on the loading level of MMT. A high energy of electron beam may destruct the crosslinking network within polymer but also may show significant improvement on the mechanical properties MMT and ATH added LDPE-EVA where amount of MMT shows high effect on crosslinking.

2.6 Scanning Electron Microscopy (SEM) Analysis

At Section 2.5, the samples are fractured after tensile testing. From the fractured samples, its fractography can be studied using microscopy. There are many available microscopy technique that can used for studying the fractured surface morphology. In general, microscopy can be classified as two types which are electron microscopy and light microscopy. Their principle of visualization the surface is different. For light microcscopy, it uses visible light as sources and glass made lenses are used to do the magnification. On the other hand, electron microscopy uses electron beam as source and operates at very low pressure. Magnification for electron microscopy is performed by electromagnetic lenses (Stadtländer, 2007). Both methods has its pros and cons at different aspects. Scanning electron microscopy (SEM) and transmission electron microscopy (TEM) are categorized as electron microscopy. SEM, TEM and light microscopy has their pros and cons at different aspects.

First, discuss the differences between SEM and TEM. In SEM analysis, electrons are emitted to the samples and samples regenerate secondary electrons which will be collected by system generating a 3-D image with the aid of software. For TEM microscopy, the samples used must be very thin. Next, the electron will be radiated and then pass through the thin samples. With the help of computer, a 2-D image will be generated. In addition, SEM and TEM have different range for magnification. The magnification range of TEM is about five times larger than the SEM's magnification range but the preparation step for TEM analysis is more than SEM (Stadtländer, 2007).

The difference between SEM and optical microscopy has been discussed by Borel, Ollé, Vergès and Sala in 2014. The most obvious difference is the image generated by optical microscopy has colour similar to samples viewed by our bare eyes whereas the image from SEM is black colour only. SEM can magnify the samples larger than optical microscopy. In addition, optical light microscopy may have focus problem to capture the image whereas SEM does not need to focus. Besides that, the preparation of SEM is required to coat a thin good conductivity material on the surface of the sample. This step is costly because the material used for coating is gold or carbon.

By comparison the three microscopy method above, it can be said SEM is more convenient to use for studying fractography in this project. The step for SEM must be conducted well in order to get a good outcome from each analysis. The preparation step can be divided into 8 steps:

1) Surface cleaning: To remove the deposits or contaminants from the surface which going to be observed in order to obtain a better visual on the surface.
2) Samples fixation: To prevent the sample moving during testing by adding chemical fixatives.
3) Removing of excess fixative: To remove excess chemical deposited by rinsing with buffer.
4) Dehydrating the sample: To remove the water molecule.
5) Drying the sample: Sample must be dried to be able operate in vacuum environment or else the sample will be destroyed.
6) Mounting the sample: Mount the sample on the SEM holder at a good orientation.

7) Sample coating: A good electrical conductivity layer is used to coat the surface of the fracture.
8) Analyse the specimen
(Stadtländer, 2007)

Bee, et al. (2013) has studies the morphology of ATH and MMT added LDPE-EVA blends. In their journal, they state that formation of fibrils or discontinuous phase is lesser and thinner for irradiated sample. The development of fibrils is due to the stress created during tensile test. The reason why irradiated sample has lower development of fibrils and thinner fibrils is because crosslinking is able to improve the polymer resistivity to stretching. Besides that, they also found that 250 kGy of high irradiation dosage can cause accumulation of fillers particles.

The morphology regarding to MOH composites has been considered by Liu (2014). Through SEM, Liu observes that numerous holes and granular MOH combine and present at the fracture surface of LDPE/MOH and XLPE/MOH blends. This condition can be related to the bonding between LDPE or XLPE with MOH is not strong and contribute to the lower tensile strength and elongation at break.

2.7 Limiting Oxygen Index (LOI) Test

As stated in fire triangle, there are three components must exist together in order to cause a fire. The components are fuel, heat and oxygen. In other word, one of the way to control the fire is to adjust the oxygen level in the environment. However, concentration of oxygen is fixed at 21 %. Thus it is impossible to control the oxygen content in atmosphere but we can modify the fuel which means our polymer. Flammability of polymer can be enhanced for by adding flame retardant additives. One of the factor to consider flame resistance of a polymer is to the amount of oxygen required to support a continuous fire. Hence, limiting oxygen index test is conducted. The LOI value for pure ABS is in a range of 19 to 35 % (Whelan, 1994).

During LOI test, the experiment is carried out in a controlled mixture of oxygen and nitrogen gas. Then, the specimen is ignited at top of the sample and then adjust the concentration of oxygen in the controlled atmosphere to find at which concentration of oxygen can support the sustainable burning of polymer. The LOI is defined by the formula below:

$$LOI = \frac{[O_2]}{[O_2]+[N_2]} \times 100\ \% \tag{2.8}$$

(Suzanne, Delichatsios and Zhang, 2013)

From the value of LOI, we can differentiate the flammability level of the polymer:

a) Flammable
b) Slow Burning
c) Self-extinguishing
d) Intrinsically non-flammable

Under atmosphere condition, the air contains 21 vol% of oxygen and this value is the reference point for the researcher to refer. Any polymer has LOI which higher than this value will be considered good in fire resistance. Nelson (2002) has classified the polymer with LOI less than the reference point of 21 % is flammable. Plastics with LOI with more than 100 % is intrinsically fire resistance. In between 21 % to 100 % LOI, Nelson further divided it into two groups as slow burning and self-extinguishing. Fenimore (as cited in Nelson, 2002) categorised polymer with range of 21 % to 28 % LOI as slow burning. Thus, Nelson describe the polymer with 28 % as lower limit and 100 % as upper limit of LOI as self-extinguishing polymer (Nelson, 2002).

The value of LOI can be affected by the electron beaming. A study has been done to understand the relationship between irradiation dosage and LOI of LDPE-EVA mixed with MMT and ATH (Bee, et al., 2013). The higher the radiation emitted onto the samples, the higher the crosslinking density within polymer matrix and then induce a higher LOI. Furthermore, loading level of flame retardant fillers can help to improve the flame resistivity of the polymer. A journal (Zhang, et al., 2005) shows that the

thermal properties of samples are linearly proportional to the ATH loading level in the blend. The LOI value increase is due to the formation of insulated layer by degradation of ATH. This insulated layer prevents the oxygen to reach the polymer to sustain the fire. The formation of char insulated layer in condensed phase can be enhanced by crosslinking process because conjugated structures and aromatic rings are formed during combustion (Bee, et al., 2013). The effect of zinc borate on LOI of composites can refer to the research done by Mergen, et al. (2012). They compare the pure PVC, 1 wt% zinc borate added PVC composite and 5 wt% zinc borate added PVC composite. Once zinc borate is added to PVC matrix, it will evaporate vapour and then residue boron oxide will then form a protective layer from heat and mass transfer. Hence, the more zinc borate added, the more higher the LOI of polymer.

2.8 Gel Content Test

During the preparation for sample, crosslinking is used to improve the mechanical properties of ABS/flame retardants blend by binding the linear polymers together but there is no all linear polymers is connected. Hence, crosslinked ABS/flame retardants blend will be determined for its crosslinking density using gel content test. There are two polymer groups will present at the end of gel content test. When samples are treated by solvent, the polymers which do not perform crosslinking is soluble in solvent and will be removed with solvent from crosslinked polymer. This soluble linear polymer is sol. The crosslinked polymer is called gel. This is sol-gel system. (Fouassier, 1993). The relationship between sol and gel can be described by the Figure 2.6. As gel fraction increases, sol fraction decreases.

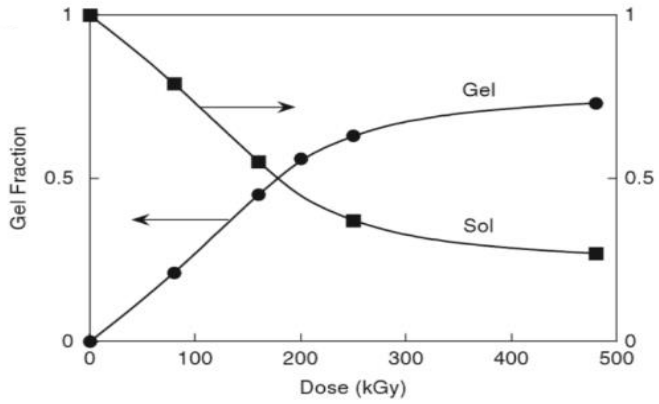

Figure 2.5: A typical example of sol-gel curve (Makuuchi and Cheng, 2012)

The crosslinking density can be measured from this formula:

$$\text{Gel Content Percentage (\%)} = \frac{W_A}{W_B} \times 100\ \% \tag{2.9}$$

Where W_A is weight of remaining sample (gel) after treatment by solvent;

W_B is weight of initial sample (sol + gel).

(Bee, et al., 2012)

High gel content percentage means there are less sol and more gel. In other way, it represents there is more crosslinked polymer than uncrosslinked polymer in the sample. Hence, the sample has high crosslinking density and will have a better properties in thermal and mechanical properties.

As shown in a study (Bee, et al., 2013), the change in irradiation dosage can significantly alter the crosslinking density of the composites. The study shows that gel content is greatly increasing in a range of 0 to 150 kGy. Nevertheless, high 250 kGy irradiation induce a relatively small rise in gel content. This is because the available volume for crosslinking is very less and crosslinking density is very high. In addition, ATH added composites can reach saturation point of crosslinking faster than MOH added composites. This results the gel content of ATH added composites steps up faster than MOH added composites (Sabet, Hassan and Ratnam, 2012).

CHAPTER 3

METHODOLOGY

3.1 Materials and Apparatus

In this study, acrylonitrile-butadiene-styrene (ABS) with grade of ABS 700314 were purchased from Toray Plastic (Malaysia) Sdn. Bhd. ABS were used as polymer base in this study. Alumina trihydrate (ATH) and magnesium hydroxide (MOH) are used as primary flame retardant filler. Alumina trihydrate with grade of Aluminium Trihydrate AL203 (64-65% purity) were supplied by KAS Aluminium (M) Sdn. Bhd. while magnesium hydroxide with technical grade were supplied by Taiko Marketing Sdn. Bhd. Furthermore, the zinc borate with flame retardant grade will be supplied by JJ-Degussa Chemicals (M) Sdn. Bhd.

The apparatus used in this study were Brabender mixer, electron beam accelerator, hot press machine, dumbbell cutter, tensile tester, scanning electron microscopy, limiting oxygen index chamber and gel content tester. Furthermore, a digital calliper was also used to measure the dimension of samples before tensile testing. Table 3.1 shows the model for the apparatus.

Table 3.1: Model of Apparatus

Apparatus	Model
Brabender mixer	Brabender® Plasti-Corder® Lab-Station
Electron beam accelerator	IMPELA 10/50
Hot press machine	YX-1200
Dumbbell cutter	Cometeh QC-603A
Digital calliper	3C301
Tensile tester	Instron 5582
Scanning electron microscopy	JEOL model JSM-6301F
Limiting oxygen index chamber	Govmark OI-1 110V 50/60HZ

3.2 Sample Preparation

The flame retarded ABS composites were prepared using Brabender mixer of Brabender® Plasti-Corder® Lab-Station in according to Table 3.2. The ABS and other fillers were compounded in Brabender mixer at the heating temperature of 180˚C and rotor speed of 50 rpm. The samples were compounded for a mixing time of 12 minutes.

Table 3.2: Formulation with fixed ABS and ATH with variation on zinc borate and fixed ABS and MOH with variation on zinc borate

Materials	Loading level, phr				
ABS	100	100	100	100	100
ATH	80	80	80	80	80
Zinc borate	0	5	10	15	20
ABS	100	100	100	100	100
MOH	80	80	80	80	80
Zinc borate	0	5	10	15	20

The compounded samples were compression moulded into 1 mm thickness sheet by using YX-1200 hot press machine under heating temperature of 155 ˚C.

Before the compression moulding process, the compounded samples were preheated under heating temperature of 150 ˚C for 5 minutes. After preheating, the preheated samples were then compression moulded into 1 mm thickness sheet at heating temperature of 180 ˚C under pressure of 10 MPa for another 5 minutes. Then, the compression moulded samples were further cooled down under pressure of 10 MPa with cooling rate of 20 ˚C /min for 3 minutes.

The 1 mm thickness sheet of samples were electron beam irradiated to 50 kGy, 100 kGy, 150 kGy, 200 kGy and 250 kGy using an electron beam accelerator with irradiation dosage of 50 kGy per pass. The accelerator model used for electron beaming was IMPELA 10/50 with 10 MeV of beam energy and 115 mA of peak beam current.

3.3 Tensile Test

The objective of tensile test was to understand the relationship between loading level of flame retardant fillers blends in ABS with their tensile strength and elongation at break. The 1 mm thickness sheets were cut into dumbbell shape in accordance to ASTM D1822. The dumbbell shape specimens were then tested under the crosshead speed of 50 mm/min and cell load of 5 kN using Instron Universal testing Machine. The tensile strength and elongation at break of all samples were taken as an average value of 5 specimens.

3.4 Scanning Electron Microscopy (SEM) Analysis

Surface morphologies of fractured samples were observed using JEOL model JSM-6301F SEM machine with a voltage of 15 kV. The fractured samples were cut into a smaller portion before conducting the scans. The cut samples were placed and mounted onto the copper stub with the fractured surface facing up. The mounted samples were

then be coated with a thin layer of gold. The samples were scanned under magnification of 1000 X, 8000 X and 15000 X.

3.5 Limiting Oxygen Index (LOI) Test

Limiting oxygen index tests were conducted using an apparatus from Rheometer Scientific, United Kingdom according to ASTM D2863. The 1 mm thickness sheets were cut into the dimensions of 50 mm × 150 mm × 1 mm and placed vertically in a transparent test column. An oxygen-nitrogen atmosphere was formed inside the test column by purging a mixture of nitrogen and oxygen. The specimens were ignited at the top with a burner. The concentration of oxygen level in the mixture gas inside the test column was adjusted until it is sufficient enough to support the combustion of specimens. Nine specimens are tested and the LOI values were taken as an average of nine specimens.

3.6 Gel Content Test

The gel content level of all flame retarded ABS composites were measured in accordance to ASTM D2765. The samples are gravimetrically immersed and heated in methyl-ethyl-ketone (MEK) at heating temperature of 80℃ for 24 hours. After extraction process of 24 hours, methyl-ethyl-ketone were used to wash the samples at least 4 times to remove the stain of soluble materials on the extracted samples. After that, the washed samples were then soaked into methanol for 20 minutes before dried to constant weight in a vacuum oven for 5 hours. The dried samples were weighed. The gel content percentage of flame retardant added ABS samples was calculated according to equation 3.1. Three specimens were conducted for each samples to obtain an average reading.

$$\text{Gel Content Percentage (\%)} = \frac{W_A}{W_B} \times 100\ \% \qquad (3.1)$$

where,

W_A = Weight of the remaining sample after extraction, g

W_B = Initial weight of the sample, g

CHAPTER 4

RESULTS AND DISCUSSIONS

4.1 Gel Content

The gel content test was performed to examine the degree of crosslinking networks formed in ABS matrix. The gel content of ATH-ABS composites increased more than 20 % when subjected to irradiation dosage of 50 kGy as shown in Fig. 1. This is due to the ionizing radiation could induce the release of polymeric free radicals to perform crosslinking to form three-dimensional network, thus reducing the solubility of the irradiated ABS composites (Bee, et al., 2013 and Landi, 2003). When higher irradiation dosages (> 100 kGy) subjected to all ATH-ABS composites, the gel content of the ATH-ABS composites (except > 5 phr) started to decrease. This is because benzene ring of styrene could prevent the crosslinking effect inside ABS matrix by hindering the transport ability of polymeric free radicals inside polymer matrix. Besides that, Pentimalli, et al. (1996) also stated that aromatic structures had resistance to crosslinking effect as this phenyl rings provided both an intra- and inter- molecular protecting effect. Therefore the gel content results did not continue to increase but in fact it showed decreasing trend. The decreasing of gel content could be due to the degradation of butadiene. There is a report stating the butadiene degrade as irradiation dosage above 100 kGy (Sterigenics [no date]). In addition, the high irradiation energy breaking the stable benzene ring. When benzene rings break down, the crosslinking bonds around the benzene rings are destructed; reducing the crosslinking density and gel content. Furthermore, the 5 phr ZB added ATH-ABS composites was observed to have higher resistance to the destruction of high irradiation energy because its gel content started to decrease at 200 kGy. Moreover, the decreasing of gel content results

were observed to revert its trend to inclination trend. This is because the breakdown of benzene ring producing linear polymeric free radicals to perform the crosslinking effect causing gel content of ATH-ABS composites to increase. Furthermore, at highest irradiation dosages (250 kGy), the gel content of non-added ATH-ABS composite showed a fall in gel decreased but the ZB added ATH-ABS composites showed an inclination trend in gel content result. This indicates the presence of ZB able to help ATH-ABS composites to sustain high irradiation energy (at 250 kGy) and prevent chain scissioning within ABS matrix.

The effect of ZB loading level on gel content result of ATH-ABS composites under various irradiation dosages was showed in Figure 4.1. For un-irradiated and 50 kGy irradiated ATH-ABS composites, the higher ZB loading level added ATH-ABS composites induced a higher gel content percentage than un-added and 5 phr ZB added ATH-ABS composites. It was believed the ZB had make ATH-ABS composites to be more insoluble to Methy Ethyl Ketone (MEK) solvent. The 20 phr ZB added ATH-ABS composites gave the highest gel content percentage than other ATH-ABS composites at 0 kGy and 50 kGy irradiation dosages. However, when ATH-ABS composites irradiated at above 100 kGy, the effect of ZB loading level on composites was minor because the disturbance of benzene ring and degradation of butadiene became the primary causes to cause gel content to decrease. The 15 phr ZB added ATH-ABS composite was largely affected by the crosslink inhibitor of benzene ring and degradation of impact modifier (butadiene). Nevertheless, the non-added, 5 phr ZB added and 20 phr ZB added ATH-ABS composites had the similar crosslinking density at 100 kGy. This condition was quite rare as different loading level of fillers with different irradiation dosages could able to give the similar crosslinking density. By observing ATH-ABS composites with highest loading level (20 phr) of ZB, its gel content results were all time higher than other ZB loading level ATH-ABS composites. Furthermore, 60% gel content was the highest crosslinking density that ZB added ATH- ABS composites could achieve. Moreover, 10 phr and 15 phr ZB were examined to have a weak crosslinking effect at higher irradiation dosages (> 100 kGy).

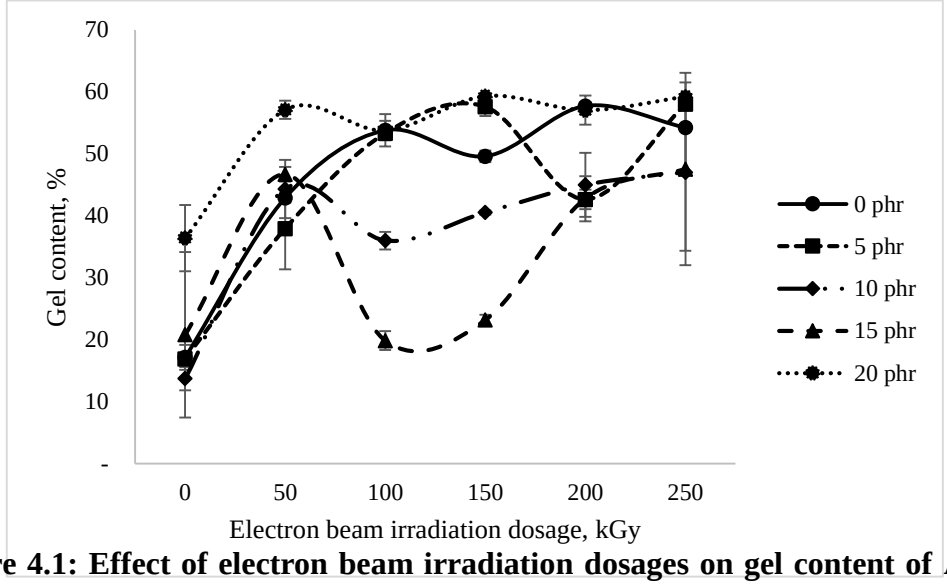

Figure 4.1: Effect of electron beam irradiation dosages on gel content of ATH-ABS composites with increasing ZB loading level.

According to Figure 4.1, the gel content of all MOH-ABS composites increased when irradiated with 50 kGy. These increments are expected because the application of electron beam irradiation on MOH-ABS composites leads to the establishment of polymeric free radicals. With these polymeric free radicals, three-dimensional crosslinking networks are formed and these networks can withstand the attack by hot MEK solvent (Bee, et al., 2013). By increasing irradiation dosage from 50 kGy to 100 kGy, the lower ZB loading level (5 phr, 10 phr and 15 phr) added MOH-ABS composites showed a decrease in gel content result. This infers the 100 kGy irradiation dosage induces the degradation of butadiene and crosslinking inhibition by benzene ring of styrene (Sterigenics, 2013). The degradation of butadiene could lead to the chain scissioning within ABS matrix; reducing the gel content of MOH-ABS composites. On the other hand, 20 phr ZB added MOH-ABS composites showed an increment in gel content as irradiation dosages increased from 50 kGy to 100 kGy but the decrement only started at 150 kGy. The 20 phr of ZB added MOH-ABS composites has the highest resistance to the solvent. Natwig (1984) used ZB as anti-erosion fillers for insulating material and then the author stated that the maximum erosion resistance effect by ZB could be achieved as its concentration was about 25 % weigh percent of the entire material. Therefore, 20 phr of ZB makes 100 kGy irradiated MOH-ABS composites to be less soluble to MEK solvent. When irradiation dosages increased from 100 kGy to 200 kGy, the gel content of ZB (except 20 phr) added MOH-ABS

composites increased showing there was improvement of crosslinking effect. The increment was due to the breakdown of aromatic ring of styrene promoted the establishment of linear polymeric free radicals which were responsible to the increment in gel content when those radicals crosslinked. Furthermore, from 100 kGy to 200 kGy, the 20 phr ZB added MOH-ABS composites underwent the degradation of butadiene followed by the formation of linear polymeric free radicals through the breakdown of benzene ring. Thus, the gel content of 20 phr ZB added MOH-ABS composites decreased at 150 kGy and increase back as irradiation dosages used was 200 kGy. Subsequently, the gel content of all ZB added (except 20 phr) MOH-ABS composites decreased when the composites were irradiated at 250 kGy. This might due to the high irradiation energy causes chain scission within ABS matrix. The non-ZB added MOH-ABS composites had a gradually increase in gel content along the increasing of electron beam irradiation dosages.

As shown Figure 4.2, the value of gel content were affected by the ZB loading level of MOH-ABS composites with different irradiation dosages. The un-irradiated and 50 kGy irradiated MOH-ABS composites added with 20 phr ZB had the lowest gel content. When the composites were irradiated at 100 kGy, the gel content of 20 phr ZB added MOH-ABS composites was higher than the gel content of lower ZB loading level (5 phr, 10 phr and 15 phr) added MOH-ABS composites. At 100 kGy, the butadiene within ABS matrix started to degrade causing crosslinking network to be destroyed and the gel content of lower ZB loading level to decrease whereas 20 phr ZB added MOH-ABS composites had not yet show the sign of degradation of butadiene (Sterigenics, 2013). The similar condition occurred at 150 kGy. At 150 kGy, the 20 phr ZB added MOH-ABS composites encountered a decrease in gel content whereas the lower ZB loading level added MOH-ABS composites was observed to have an improvement on crosslinking effect. The improvement of crosslinking effect at 150 kGy was believed due to the breakdown of aromatic ring of styrene promoting the formation of three-dimensional crosslinking network by the linear polymeric free radicals from aromatic ring.

In general, the increasing of electron beam irradiation dosages increased the crosslinking density of ATH-ABS and MOH-ABS composites. Nevertheless, the degradation of butadiene gives negative effect on the crosslinking network whereas

the breakdown of benzene ring improve the crosslinking network of the composites. Furthermore, high irradiation energy from electron beam accelerator would cause chain scissioning within ABS matrix; reducing the gel content percentage of the composites (Bee, et al., 2013).

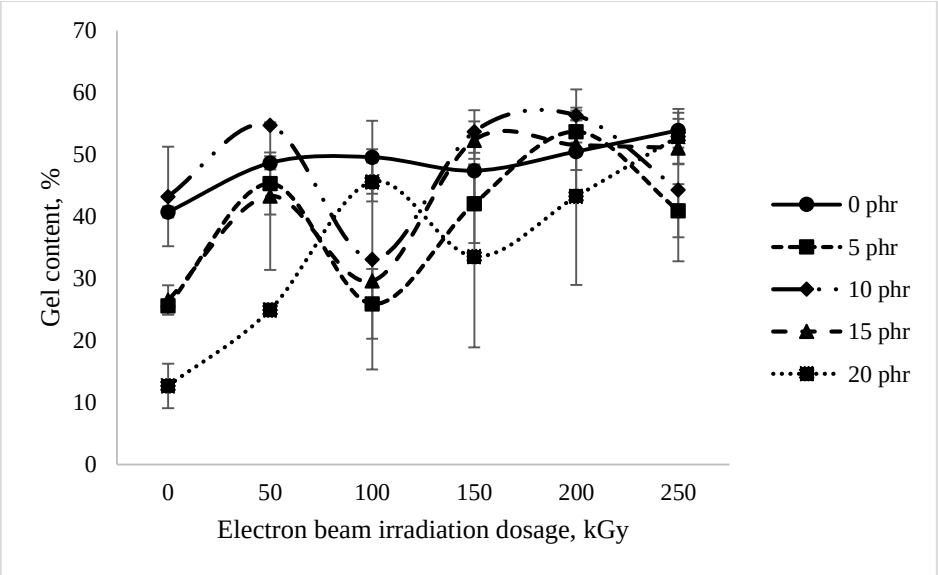

Figure 4.2: Effect of electron beam irradiation dosages on gel content of ABS added with MOH and increasing ZB loading level.

4.2 Mechanical Properties

According to Figure 4.3, the effect of alternating ZB loading level in ATH-ABS composites on its tensile strength was studied. As loading level of ZB increased from 0 phr to 5 phr, the irradiated ATH-ABS composites had a decreasing tensile strength result. The decreasing in the tensile strength with an increasing loading level of ZB had been studied by Mergen, et al. (2012) and Yidiz, Seydibeyoğlu and Güner (2009). They observed the similar mechanical influence of addition of ZB on the tensile strength. However, there are some critical parts as according to their research, the influence of addition of ZB has a minimal negative effect on tensile strength but tensile strength of irradiated ATH-ABS composites had a considerable decrement in tensile strength. The reason might be the crosslinking is a dominant factor over the addition of ZB in lowering the tensile strength of ATH-ABS composites. On the other hand,

the un-irradiated ATH-ABS composites had an improvement in tensile strength as 5 phr of ZB was added into the composites. This was contradict with the finding of Mergen, et al. (2012) and Yidiz, Seydibeyoğlu and Güner (2009). Once the ZB loading level was added to 15 phr, the tensile strength of un-irradiated and 50 kGy irradiated ATH-ABS composites had increased especially 50 kGy irradiated ATH-ABS composites showed a leap in tensile strength value. With increasing of ZB loading level from 15 phr to 20 phr in un-irradiated and 50 kGy irradiated ATH-ABS composites, their tensile strength decreased significantly. It was believed that high loading level of ZB might started to become incompatible with ATH-ABS composites and hence cause reduction in tensile strength (Sain, et al., 2004). Furthermore, the significant negative effect of high ZB loading level on the tensile strength of ATH-ABS composites might be caused by the increasing of poor interaction in interfacial adhesion between fillers and matrix.

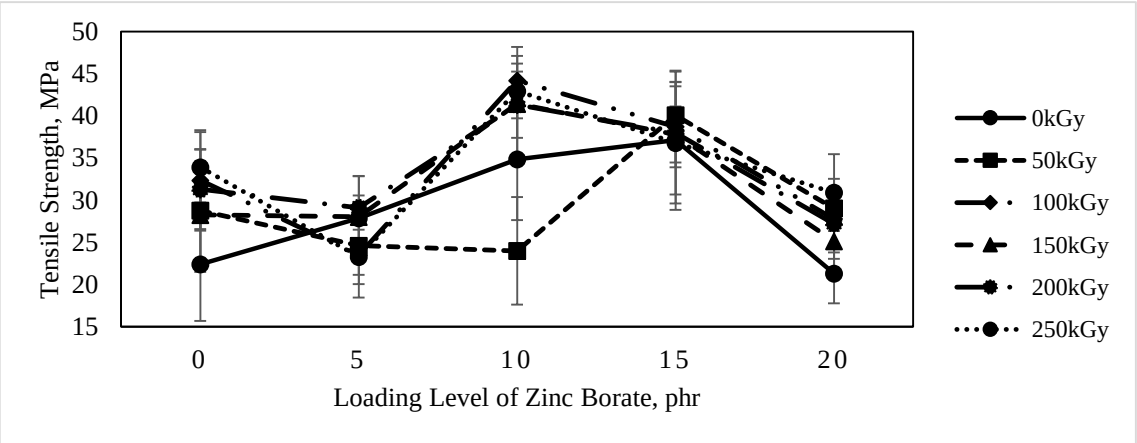

Figure 4.3: Effects of zinc borate loading level on tensile strength of ABS blended with ATH under different electron beam irradiation dosages.

The effect of irradiation dosage on the tensile strength of ATH-ABS composites was observed through Figure 4.4. When the samples were irradiated to 50 kGy, the 5 phr and 10 phr ZB added ATH-ABS composites showed a decreasing tensile strength whereas the tensile strength of non-ZB added, 15 phr and 20 phr ZB added ATH-ABS composites was improved. Subsequently, when the ATH-ABS composites were continued to be irradiated to 100 kGy, the composited compounded by 10 phr of ZB was observed to have a drastically increment in tensile strength. Besides that, the tensile strength of non-ZB added ATH-ABS composites also showed

a slightly increment. However, the other ZB loading level (5 phr, 15 phr and 20 phr) added ATH-ABS composites encountered a slightly decreasing in tensile strength. As the irradiation dosages was increased from 100 kGy to 250 kGy, 10 phr and 15 phr ZB added ATH-ABS composites stayed constantly along the increasing irradiation dosages. The tensile strength of non-ZB and 20 phr ZB added ATH-ABS composites was observed to decrease at 150 kGy and the followed by a continuous increment to 250 kGy. The decreasing in tensile strength is believed to be caused by degradation of butadiene. Nevertheless, the increment of tensile strength from 150 kGy to 250 kGy was supported by the formation of extra crosslinking network by the linear polymeric free radicals from the breakdown of benzene ring.

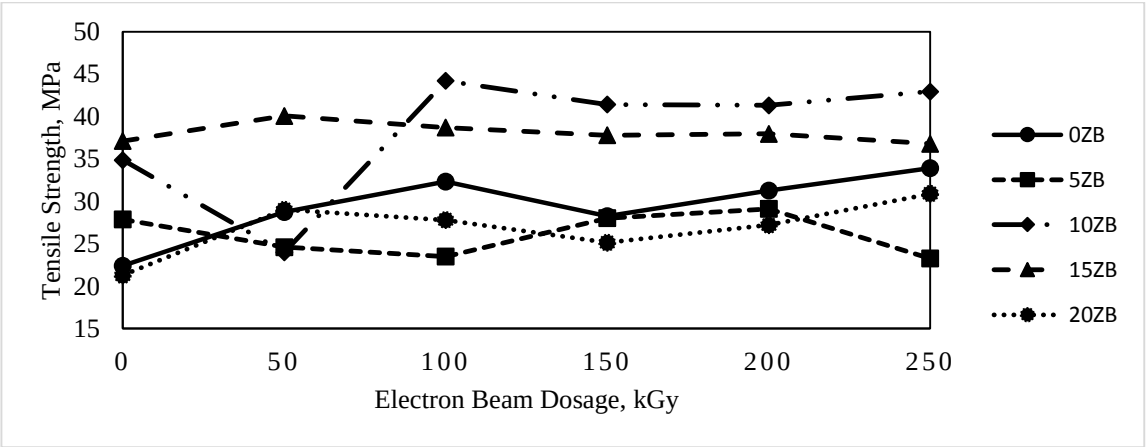

Figure 4.4: Effects of irradiation dosages on tensile strength of ABS blended with ATH under different loading level of zinc borate.

The elongation at break of ATH-ABS composites had been studied through Figure 4.5. By observing the addition of ZB from 0 phr to 15 phr, all the ATH-ABS composites (except the composites with 250 kGy) showed a slightly change in the elongation at break along with the increasing ZB loading level. The elongation at break of 250 kGy irradiated ATH-ABS composites was observed to have a drastically decreasing from above 6 % to below 1 % and then its elongation at break remained unchanged even though ZB loading level was increased to 20 phr. The considerably decrement in elongation at break is due to the high irradiation dosages might due to the high electron beam dosages destruct the crosslinking network of the higher ZB loading level (> 5 phr) added ATH-ABS composites. Furthermore, when ZB loading

level increased further to 20 phr, the elasticity of the un-irradiated and low irradiated (50 kGy and 100 kGy) decreased drastically. This might due to the increasing ZB fillers is incompatible as there is no crosslinking effect to improve the interfacial adhesion between ZB and ABS. Hence, the poor interfacial adhesion between filler and matrix makes the elongation at break of the samples to reduce. Nevertheless, high irradiation dosages like 150 kGy and 200 kGy (but not 250 kGy) able to improve the poor interfacial adhesion between ZB and matrix and the chain scission effect is still not yet the dominant to affect the elongation at break; therefore the elongation at break of the composite remains unchanged.

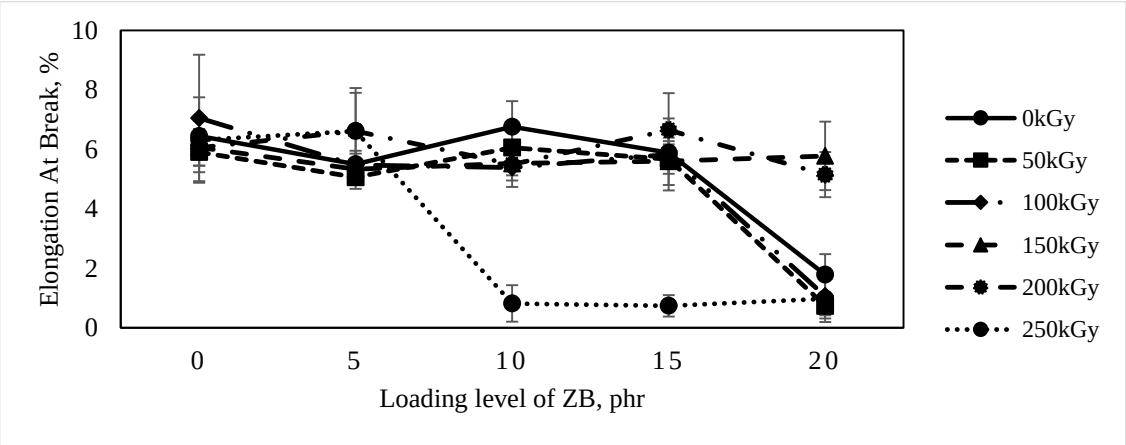

Figure 4.5: Effects of zinc borate loading level on elongation at break of ABS blended with ATH under different electron beam irradiation dosages.

Figure 4.6 at below showed the relationship between electron beam dosages and elongation at break of ATH-ABS composites with different loading level of ZB. When the irradiation dosage increased from 0 kGy to 200 kGy, the elongation at break of all the ATH-ABS composites did not have a significant change except the 20 phr ZB added composites which had a marginal increment in its elongation at break from 1 % to 6 %. Furthermore, the high irradiation dosages irradiated ATH-ABS composites had caused the elongation at break of the composites to decrease. The decrement of elongation at break could be explained through studies done by Bee, et al. (2013). In their studies, the resistance of slippage between macromolecules chain created by crosslinking network reduced the elongation at break of the composites.

.

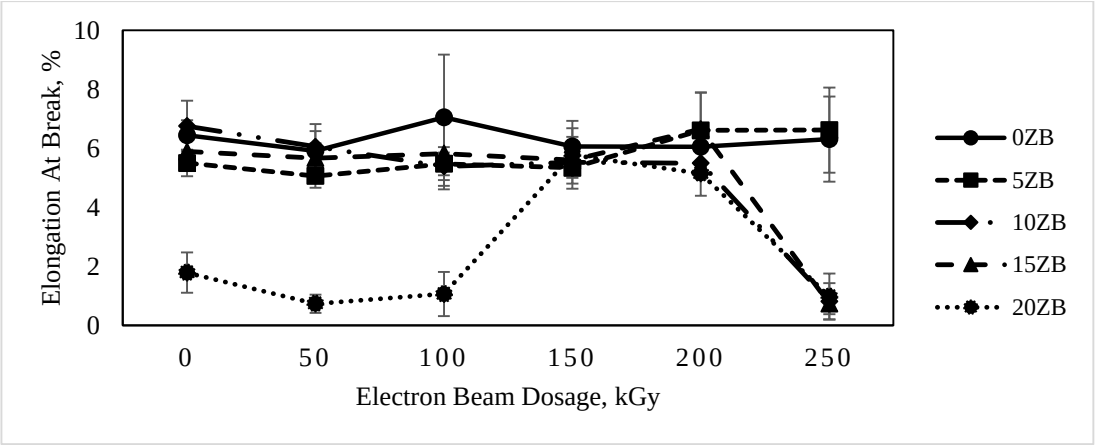

Figure 4.6: Effects of irradiation dosages on elongation at break of ABS blended with ATH under different loading level of zinc borate.

The relationship between Young Modulus with loading level of ZB of different irradiation dosages was shown in Figure 4.7. By increasing ZB loading level from 0 to 5 phr, ATH-ABS composites with different irradiation dosage had slightly decreased in Young Modulus When the loading level of ZB was further increased to 10 phr, all ATH-ABS composites showed increment in Young Modulus especially the composites with higher irradiation dosages (100 kGy, 150 kGy, 200 kGy and 250 kGy). However, the Young Modulus of ATH-ABS composites with higher irradiation dosages decreased marginally as ZB loading level was increased from 10 phr to 20 phr. On the other hand, un-irradiated ATH-ABS composites did not show significant changes with the increasing ZB loading level. Furthermore, the Young Modulus of 50 kGy irradiated ATH-ABS composites showed increment as ZB loading level increased from 10 to 15 phr and then decreased as 20 phr ZB was added into the composites.

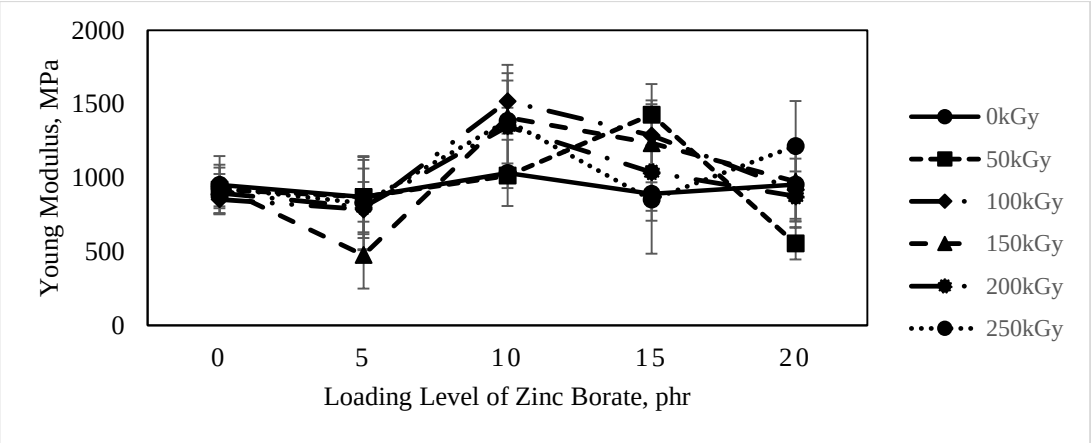

Figure 4.7: Effects of zinc borate loading level on Young Modulus of ABS blended with ATH under different electron beam irradiation dosages.

The effect of electron beam irradiation dosages on Young Modulus of ATH_ABS composites had shown in Figure 4.8. With the increasing of irradiation dosages from 0 kGy to 250 kGy, the Young Modulus of 0 phr ZB added ATH-ABS composites remained flat along the increment of irradiation dosages. Furthermore, the Young Modulus of ATH-ABS composites which blended with 5 phr ZB remained unchanged but encountered a significant decrement at 150 kGy. After that, the Young Modulus was rising back to the value around 800 MPa. ForATH-ABS composites blended with 10 phr of ZB had a leap of Young Modulus value from 50 kGy to 100 kGy and then remained above 1400 MPa until 250 kGy. Moreover, for ATH-ABS composites added with 15 phr of ZB, its Young Modulus increased drastically as irradiation dosages increased from 0 to 50 kGy. After 50 kGy, the Young Modulus slowly decreased with increasing in irradiation dosages. In addition, the ATH-ABS composites blended with 20 phr of ZB encountered a 60 % decrement in Young Modulus as the irradiation dosages changed from 0 to 50 kGy and it increased back to be above 900 MPa. Afterwards, its Young Modulus did not change much until 200 kGy but the high irradiation dosages of 250 kGy increased the stiffness of the 20 phr ZB added sample.

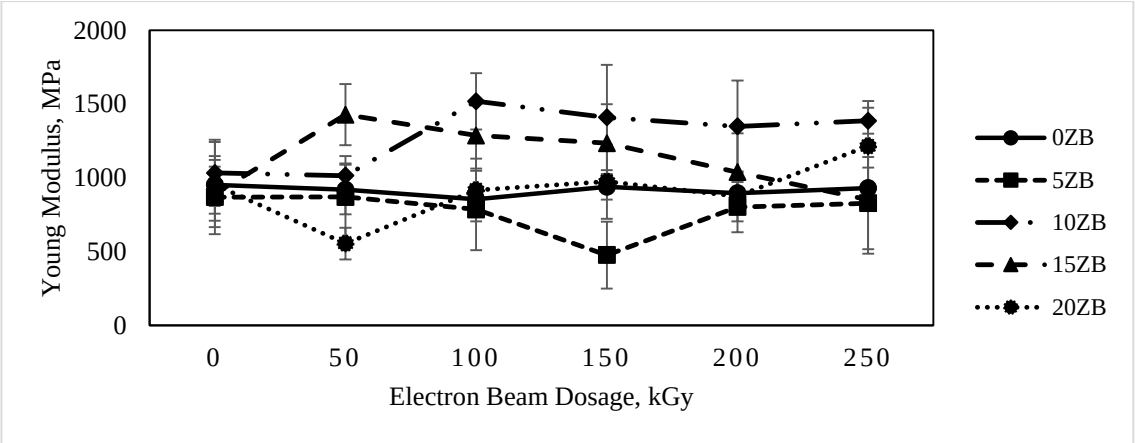

Figure 4.8: Effects of electron beam irradiation dosages on Young Modulus of ABS blended with ATH under different loading level of zinc borate.

The result of tensile strength of MOH-ABS composites affected by ZB loading level was shown in Figure 4.9 at below. When loading level of ZB increased from 0 phr to 5 phr, the tensile strength of the un-irradiated and those with higher irradiation dosages (150 kGy, 200 kGy and 250 kGy) MOH-ABS composites decreased slightly whereas the composites which irradiated at lower irradiation dosages such as 50 kGy and 100 kGy had showed some increment in tensile strength. The increasing of ZB loading level in the 150 kGy, 200 kGy and 250 kGy irradiated MOH-ABS composites caused the tensile strength of the blends to decrease because the high irradiation dosages degraded the compostes as chain scissioning destructed the crosslinking network within ABS marix; thus reducing its mechanical properties. As the loading level of ZB increased from 10 phr to 20 phr, all MOH-ABS composites showed improvements in tensile strength. The finding is conflicting with the study by Basfar (2003) which stating the increasing of ZB within the matrix could slightly increase the tensile strength of MOH added samples.

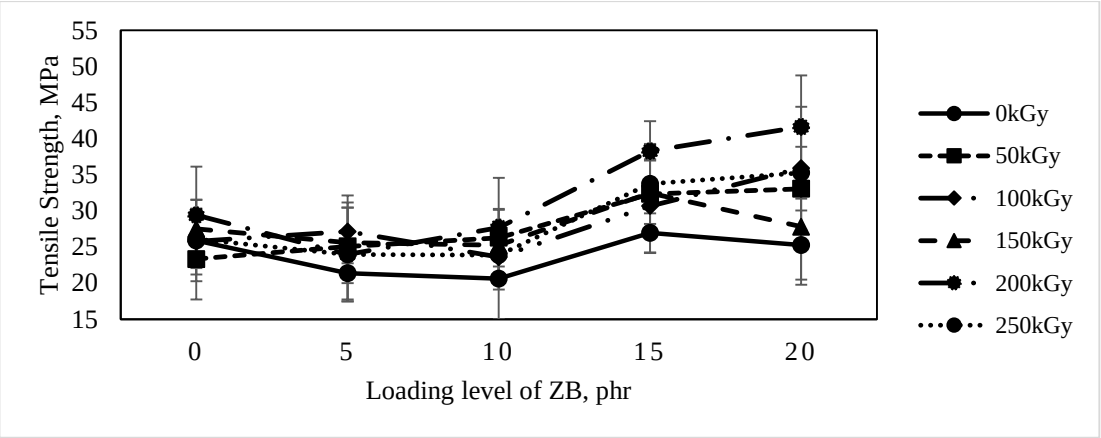

Figure 4.9: Effects of zinc borate loading level on tensile strength of MOH added ABS samples under different electron beam irradiation dosages.

Figure 4.10 at below showed how the tensile strength of MOH-ABS composites affected by electron beam dosages on different ZB loading level. All ZB added MOH-ABS composites had an increment in tensile strength as irradiation dosages changed from 0 kGy to 50 kGy. Only the tensile strength of non-ZB added MOH-ABS composites decreased. Subsequently, the non-ZB added, 5 phr ZB added and 20 phr ZB added MOH-ABS composites had an increasing tensile strength as irradiation dosages had increased from 50 kGy to 100 kGy whereas the 10 phr ZB and 15 phr ZB added composites showed a decrease in Young Modulus. When irradiation dosages continued to increase to 150 kGy, the mechanical properties of 5 phr and 20 phr ZB added MOH-ABS composites decreased whereas the other composites showed an increment in tensile strength. Moreover, the increasing of electron beam dosage could increase the tensile strength of the composites as irradiation dosages increased from 150 kGy to 200 kGy. This is because the higher irradiation dosage able to induce more free radicals in the composites to form a larger crosslinking network which contributes to a higher tensile strength (Bee, et al., 2013). Furthermore, when the electron beam dosage started to change from 200 kGy to 250 kGy, the mechanical properties of MOH-ABS composites started to decrease due to the degradation by high irradiation energy because high irradiation energy could cause chain scission to happen.

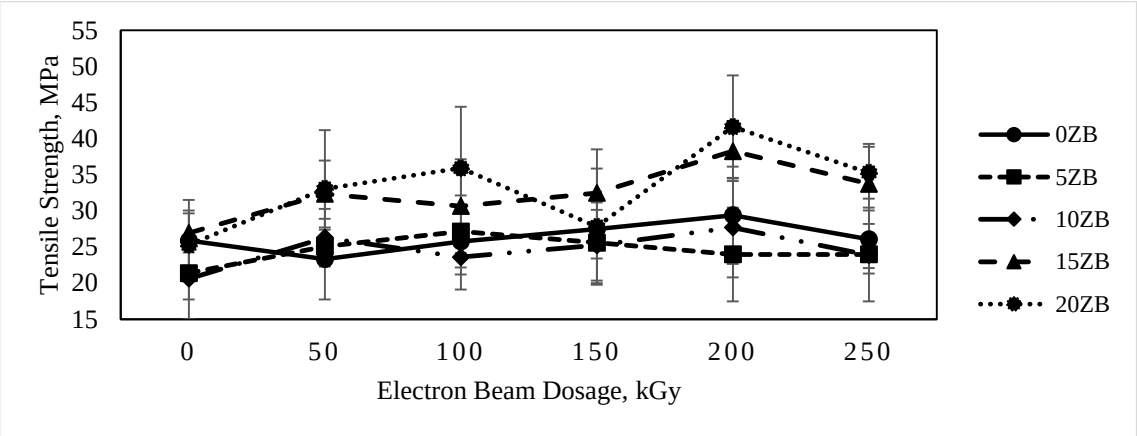

Figure 4.10: Effects of electron beam dosage on tensile strength of MOH added ABS samples under different loading level of zinc borate.

As shown in Figure 4.11, the elongation at break of MOH-ABS composites decreased with the increasing loading level of ZB. By observing un-irradiated MOH-ABS composites elongation at break results in Figure 4.11, its elongation at break decreased drastically once ZB added into the composites. The ZB in un-irradiated MOH-ABS composites might not compatible with the matrix. The incompatible between ZB and matrix makes composites had a lower ability to elongate and creates a lot of weak point for stressing. Besides that, Fang, et al. (2013) stated the addition of ZB in the composites had enhanced the rigidity of the samples; reducing the flexibility of the composites. The addition of ZB in irradiated MOH-ABS composites had also decreased the elongation at break of composites but only start to decrase when 10 phr of ZB was adding into the composites as shown in Figure 4.11.

Additionally, the elongation at break of MOH-ABS composites did not have a solid relationship with the increasing of irradiation dosages under various ZB loading level as shown in Figure 4.12. However, there were similarity between all MOH-ABS composites as irradiation dosages continued to increase. All MOH-ABS composites would undergo a cycle of decreasing and increasing in elongation at break but generally the increasing of irradiation dosages had decreased its elongation at break. This is because irradiation induced the free radicals to form three-dimensional network which prevented the structural reorganization when stress was applied. Sabet, Hassan and Ratnam (2012) also stated that the larger crosslinking network would reduce the

mobility chain; thus reduced the composites elongation at break. Furthermore, the decreasing in elongation at break might also due to the degradation of butadiene impact modifier because of high irradiation dosages (Sterigenics, 2013). However, the increasing in elongation at break was caused by the breakdown of benzene ring contributing linear polymeric free radicals. These radicals was responsible for crosslinking

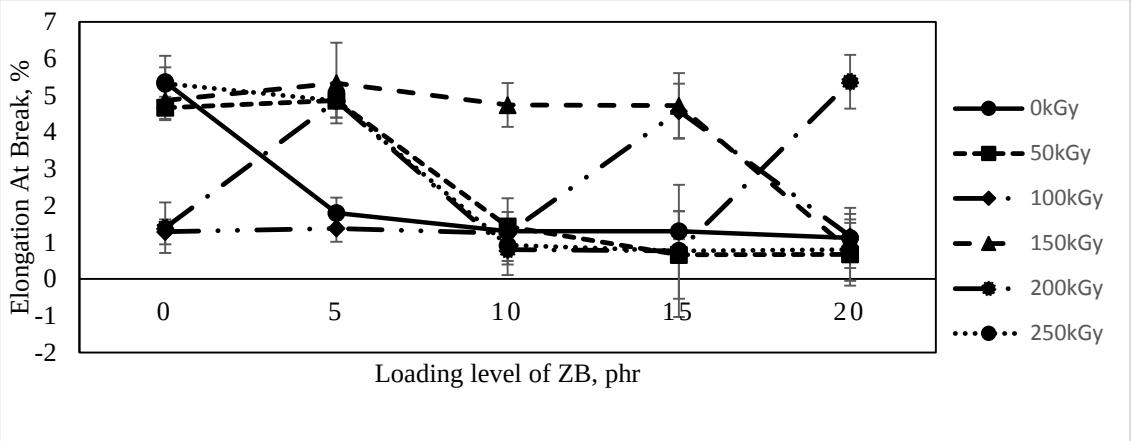

Figure 4.11: Effects of zinc borate loading level on elongation at break of MOH added ABS samples under different electron beam dosages.

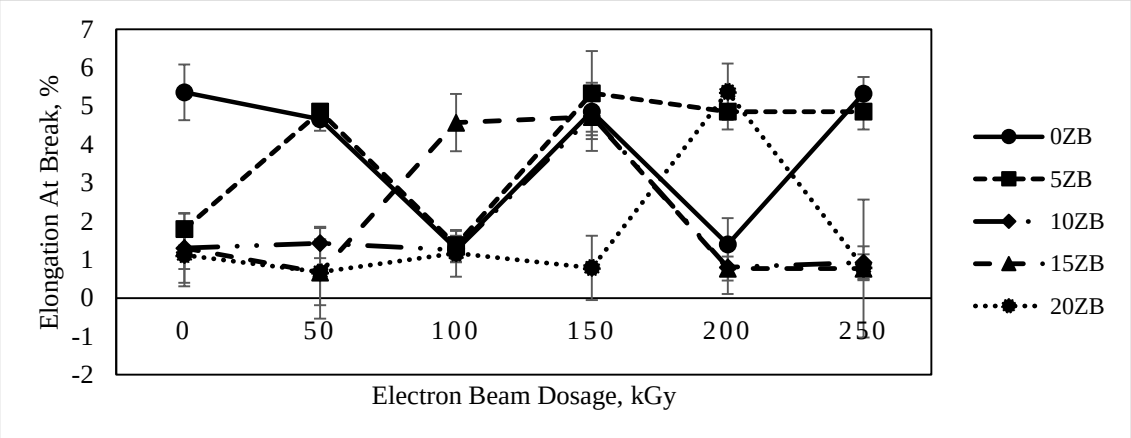

Figure 4.12: Effects of electron beam dosage on elongation at break of MOH added ABS samples under different loading level of zinc borate.

The stiffness of the composites was investigated through their Young Modulus. According to Figure 4.13, the stiffness of 100 kGy and 250 kGy irradiated MOH-ABS

composites had increased as Young Modulus of composites increased through the addition of ZB from 0 phr to 10 phr. However, the un-irradiated, 50 kGy, 150 kGy and 200 kGy irradiated MOH-ABS composites faced a gradually decreasing in stiffness as ZB loading level increasing to 10 phr. Furthermore, when ZB loading level continued to increase to 15 phr, the un-irradiated and irradiated MOH-ABS composites (except 50 kGy irradiated composites) had a drastically increase of Young Modulus. Nevertheless, at 50 kGy and 250 kGy, the stiffness of MOH-ABS composites continued to increase when 20 phr of ZB was added to the MOH-ABS composites whereas the composites with other irradiation formulation encountered reduction in stiffness.

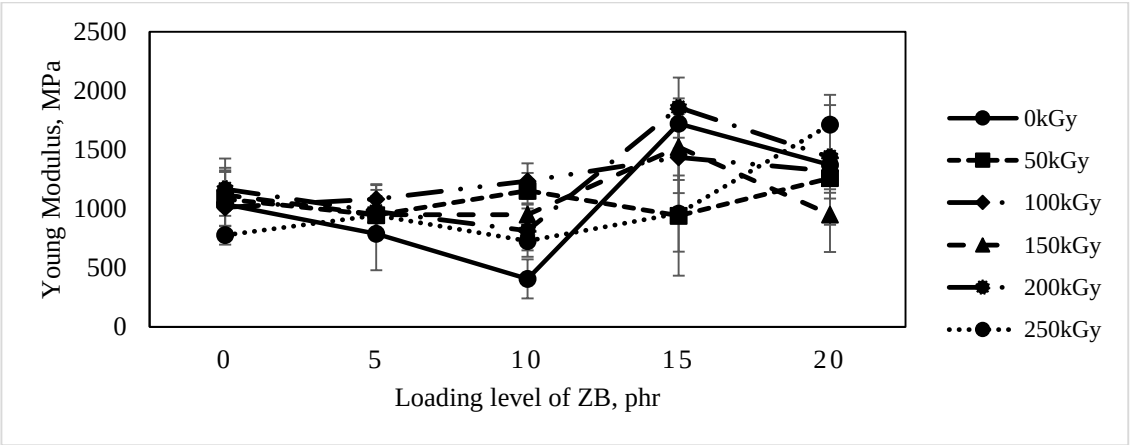

Figure 4.13: Effects of loading level of zinc borate on Young Modulus of MOH added ABS samples under different electron beam dosages.

Figure 4.14 showed the relationship between electron beam dosage and Young Modulus of the MOH-ABS composites. By looking on 0 phr of ZB added MOH-ABS composites, its Young Modulus remained around 1000 MPa and then started to increase from 100 kGy to 200 kGy followed by a significant decrement in Young Modulus at 250 kGy. Moreover, the MOH-ABS composites blended with 5 phr of ZB did not have significant changes with increasing electron beam dosage. Furthermore, the Young Modulus of 10 phr ZB added MOH-ABS composites increased as irradiation dosages increased from 0 kGy to 100 kGy. Subsequently, Young Modulus of 10 phr ZB added MOH-ABS composites gradually decreased after 100 kGy. Besides, the MOH-ABS composites added with 15 phr of ZB had a decrement of

Young Modulus with an increasing irradiation dosages from 0 kGy to 50 kGy. After that, when irradiation dosages was increased from 50 kGy to 200 kGy, the composites Young Modulus also gradually but it decreased when it was irradiated at 250 kGy. In addition, the MOH-ABS composites compounded with 20 phr of ZB had a constant Young Modulus as the electron beam dosage increased from 0 to 100 kGy and then followed by a decreasing in Young Modulus at 150 kGy. Afterwards, the Young Modulus of 20 phr ZB added MOH-ABS composites improved as the irradiation dosages increased from 150 kGy to 250 kGy. Generally, Young Modulus of MOH-ABS composites increased with the increasing irradiation dosages and loading level of ZB.

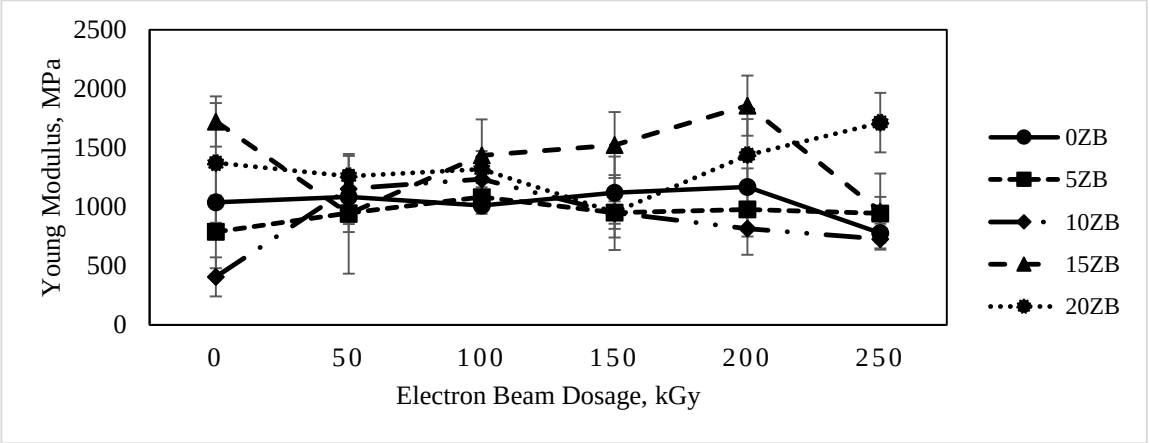

Figure 4.14: Effects of electron beam dosage on Young Modulus of MOH added ABS samples under different loading level of zinc borate.

By comparing the overall mechanical properties of ATH-ABS composites with MOH-ABS composites, ATH-ABS composites had a higher tensile strength and elongation at break than MOH-ABS composites. This result contradicted with the studies by Walter and Wajer (1998) and Sabet, Hassan and Ratnam (2012). They claimed that MOH-ATH composites gave the higher tensile strength and elongation at break than similar ATH-ABS composites. The reason might be ATH had stronger adhesion forces with ABS matrices than MOH. On the other hand, ATH-ABS composites had a lower Young Modulus than MOH-ABS composites. This result was supported by the finding in Walter and Wajer (1998).

4.3 Surface Morphology

Figure 4.15 illustrates that the SEM image for un-irradiated ATH-ABS composites without adding ZB. By observing to Figure 15, the cavities can be seen within the interface of ATH particles and ABS matrix. This indicates that the poor interfacial adhesion effect between ATH particles and ABS matrix which could cause the occurrence of cavities. Zhang, et al. (2005) reported the poor adhesion quality of ATH fillers was due to its strong surface tension between fillers and matrix. Therefore, during stressing, the cavities around ATH fillers becomes weak points within the polymer matrix and easily concentrated by the stress; giving a lower value of tensile strength.

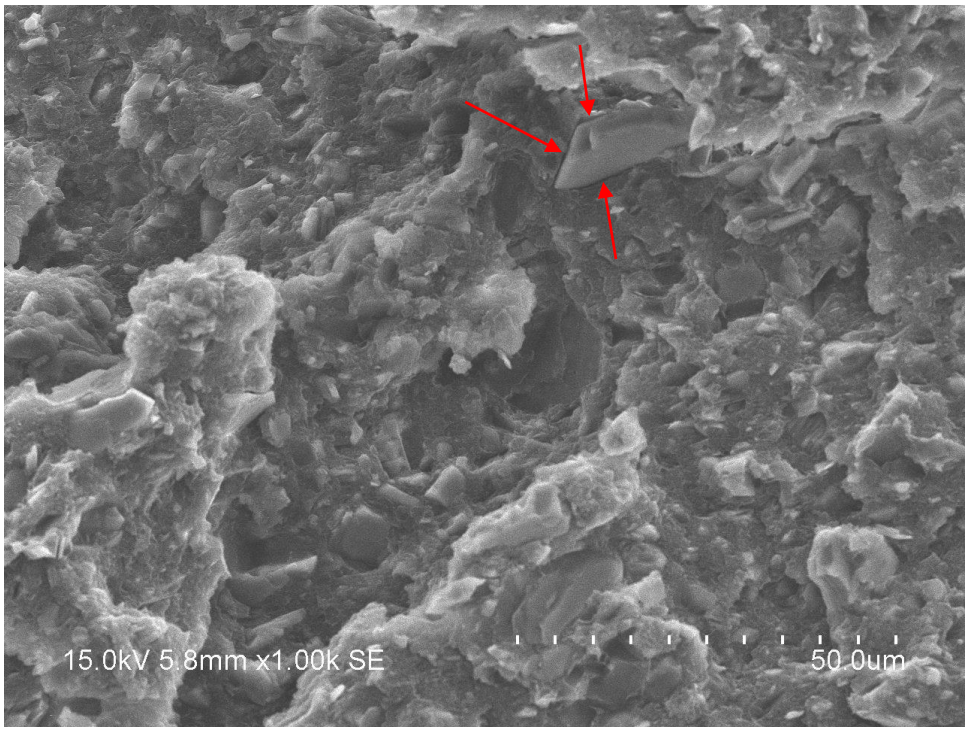

Figure 4.15: SEM micrographs of un-irradiated ATH-ABS composites with 0 phr zinc borate (ZB)

When the ATH-ABS composites with 0 phr ZB was irradiated by 50 kGy, the electron beam induced the free radicals within polymers and fillers; forming crosslinking network. By comparing Figure 4.15 with Figure 4.16, the occurrence of

cavities between the ATH particles and ABS matrix was observed to significantly reduce after irradiated up to 50 kGy.

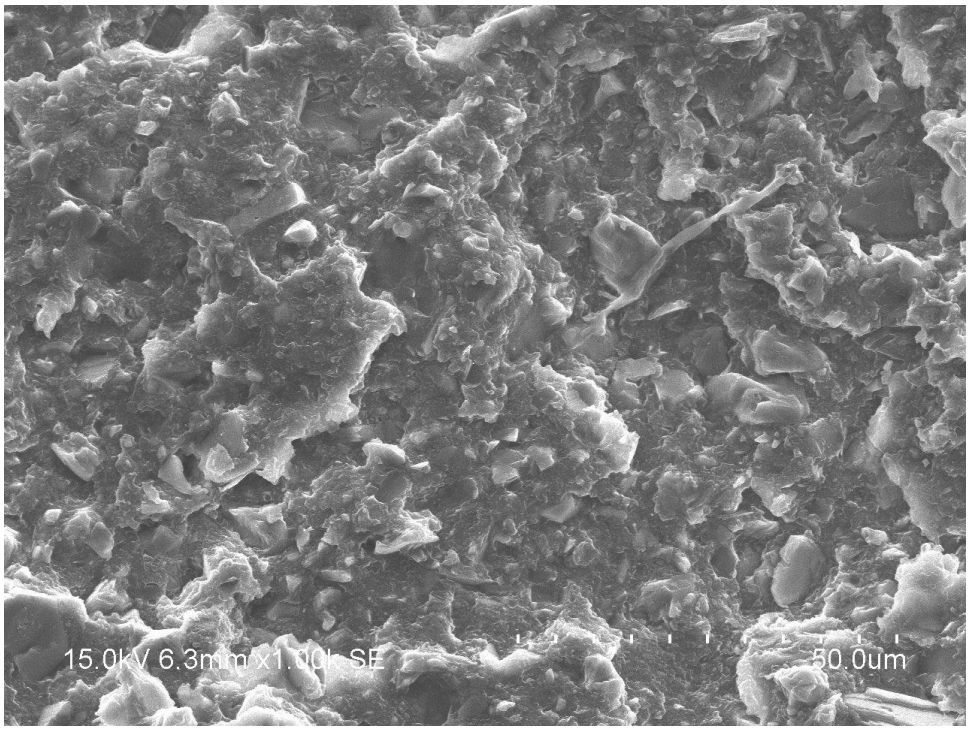

Figure 4.16: SEM micrographs of 50 kGy irradiated ATH-ABS composites with 0 phr zinc borate (ZB)

By comparing Figure 4.15 and Figure 4.16, the 150 kGy irradiated ATH-ABS composites was found to have more dis-continuous surface compared to the 50 kGy irradiated composites. The dis-continuous surfaces are due to the degradation of benzene ring and reduce the crosslinking density of the composites. Furthermore, when the ATH-ABS composites was subjected to 250 kGy, its surface was observed to have more continuous phase. This is because when the composites is subjected to high electron beam dosage the aromatic ring would breakdown. The breakdown of aromatic ring of styrene releases linear polymeric free radicals which will crosslink and then form a more continuous surface structure. By referring to the gel content (Figure 4.1) and tensile strength (Figure 4.4) results, there was a decreasing in gel content and tensile strength for 150 kGy irradiated ATH-ABS composites blended with 0 phr of ZB. Subsequently, the gel content and tensile strength of ATH-ABS composites had been improved when it was subjected to 250 kGy.

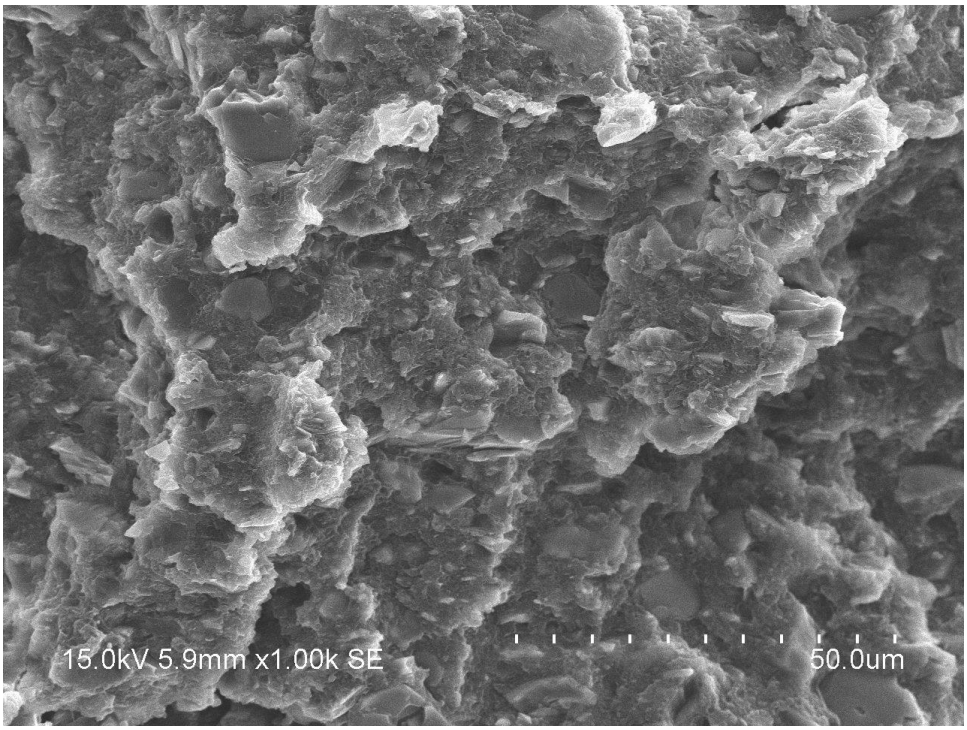

Figure 4.17: SEM micrographs of 150 kGy irradiated ATH-ABS composites with 0 phr zinc borate (ZB)

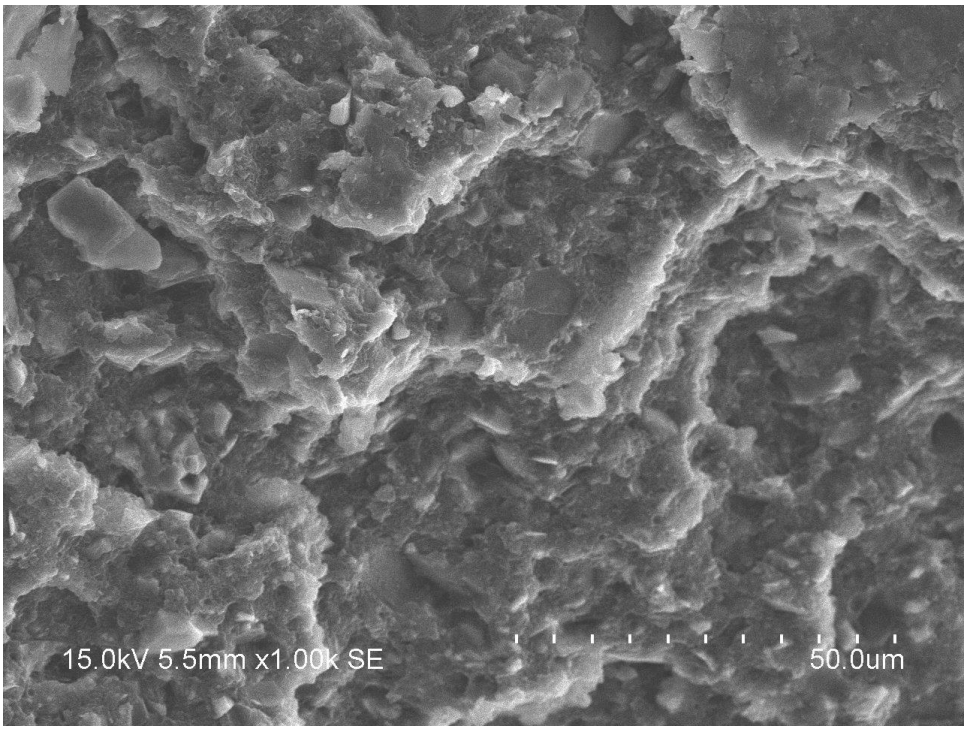

Figure 4.18: SEM micrographs of 250 kGy irradiated ATH-ABS composites with 0 phr zinc borate (ZB)

The Figure 4.19 and Figure 4.20 shown at below were the SEM morphologies of un-irradiated ATH-ABS composites which added with 5 phr and 20 phr respectively. The 5 phr of ZB added composites was observed to be distributed homogeneously throughout the matrix. However, the 20 phr of ZB added composites formed some agglomerates as shown in Figure 4.20. On the other hand, the agglomerates have a higher cavity which will force stress to concentrate on those cavities as week point. Thus the tensile strength of the 20 phr ZB added ATH-ABS composites was lower compared with other ZB loading level added composites (as shown in Figure 4.4).

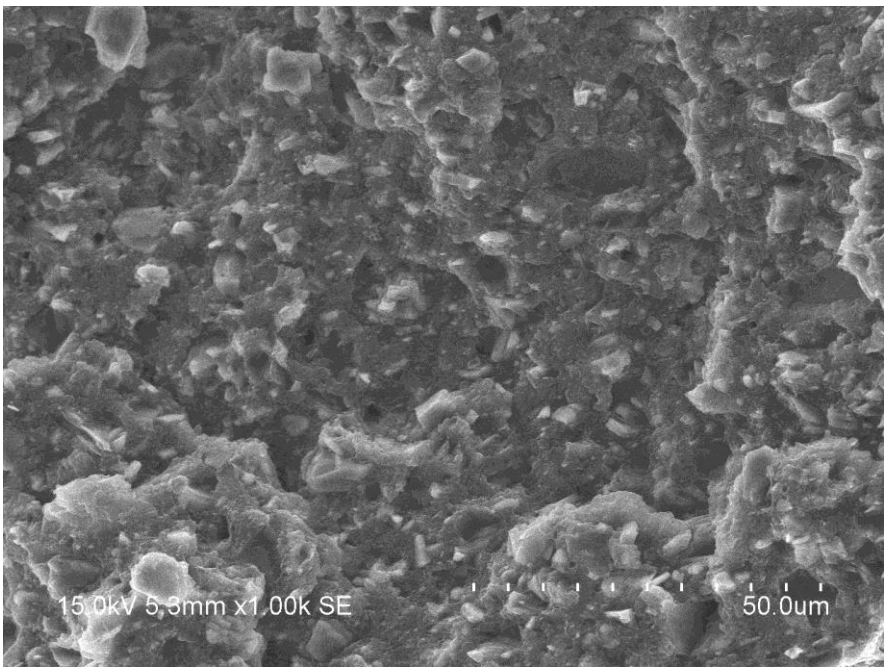

Figure 4.19: SEM micrographs of un-irradiated ATH-ABS composites with 5 phr zinc borate (ZB)

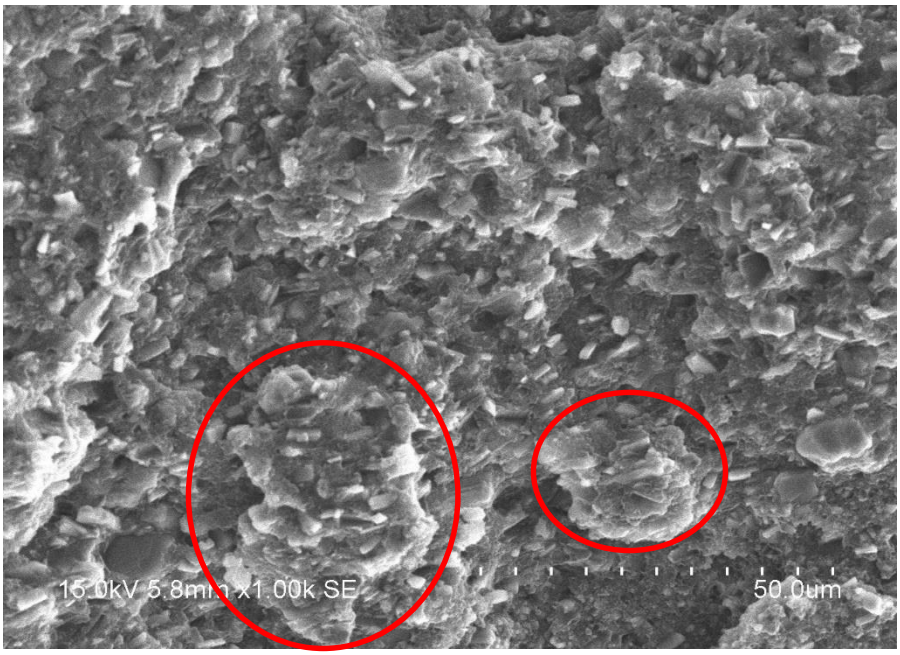

Figure 4.20: SEM micrographs of un-irradiated ATH-ABS composites with 20 phr zinc borate (ZB)

According to Figure 4.21, MOH fillers had a good interfacial adhesion with ABS matrix. The good compatible of MOH in the matrix made the un-irradiated MOH-ABS composites to have a higher tensile strength compared to the un-irradiated ATH-ABS composites (without added with any ZB). Furthermore, the addition of crosslinking effect had significantly degraded the non-ZB added MOH-ABS composites. By referring to Figure 4.22, there were plenty of bubble voids presented throughout the surfaces of composites. These bubble voids are believed to be formed by the volatile gas or water vapor produced by the degradation of ABS and MOH.

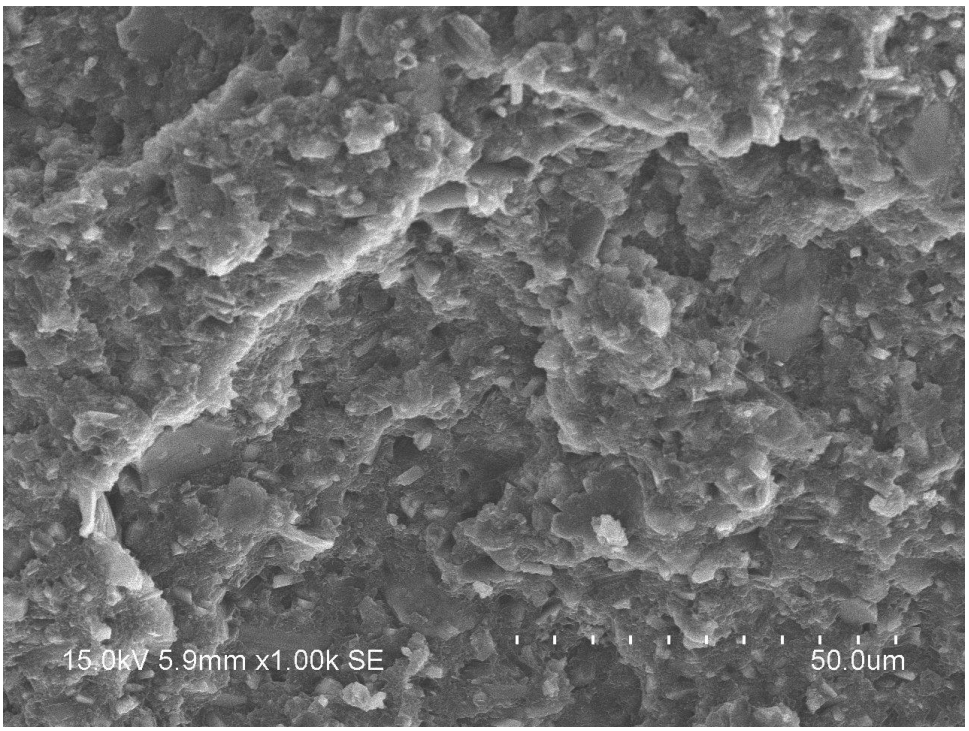

Figure 4.21: SEM micrographs of un-irradiated MOH-ABS composites with 0 phr zinc borate (ZB)

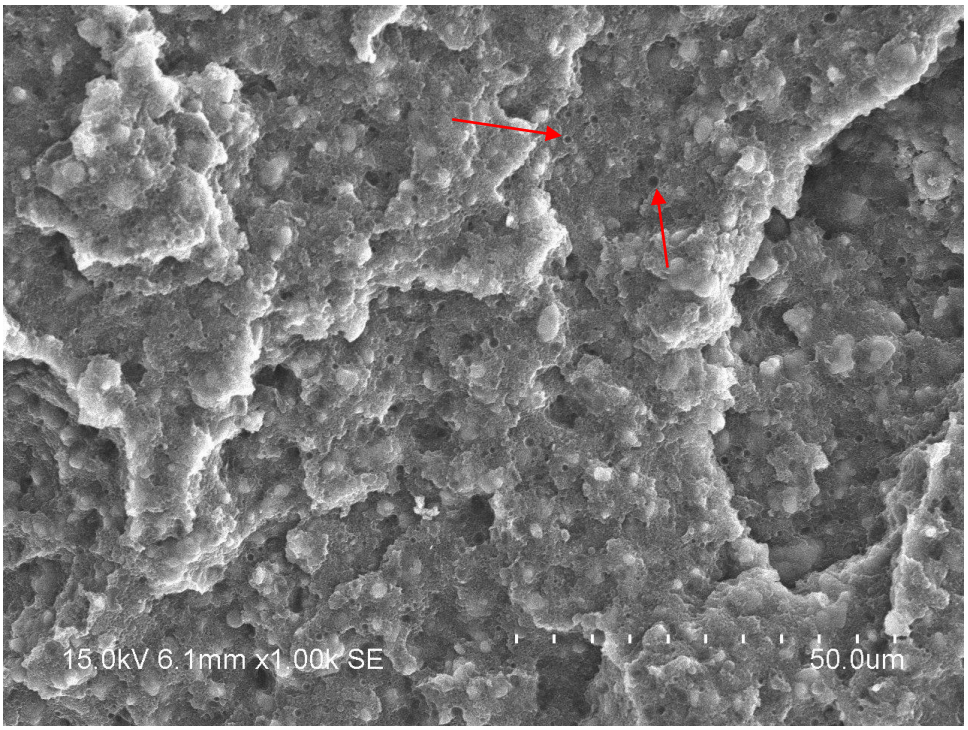

Figure 4.22: SEM micrographs of 50 kGy irradiated MOH-ABS composites with 0 phr zinc borate (ZB)

The high irradiation dosages could cause chain scission in the 20 phr ZB added MOH-ABS composites. The 150 kGy irradiated 20 phr ZB added MOH-ABS composites (as shown in Figure 4.24) had rougher surface than 50 kGy irradiated 20 phr ZB added MOH-ABS composites (as shown in Figure 4.23). This is due to the degradation of butadiene which destruct the three-dimensional of crosslinking structure which formed within the matrix when subjected to 150 kGy.

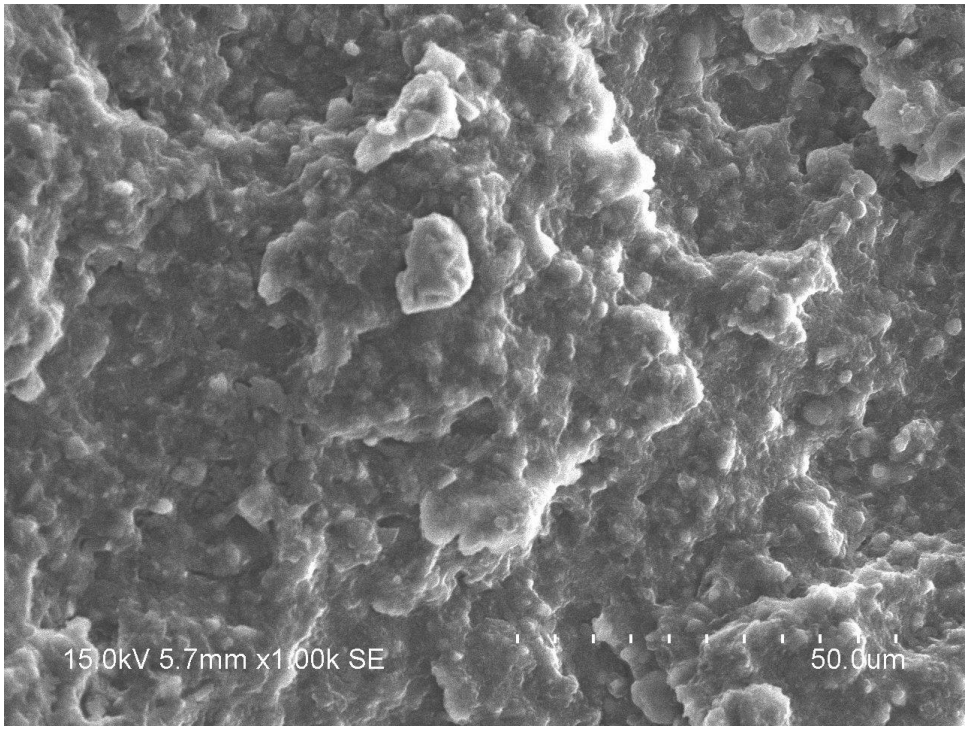

Figure 4.23: SEM micrographs of 50 kGy irradiated MOH-ABS composites with 20 phr zinc borate (ZB)

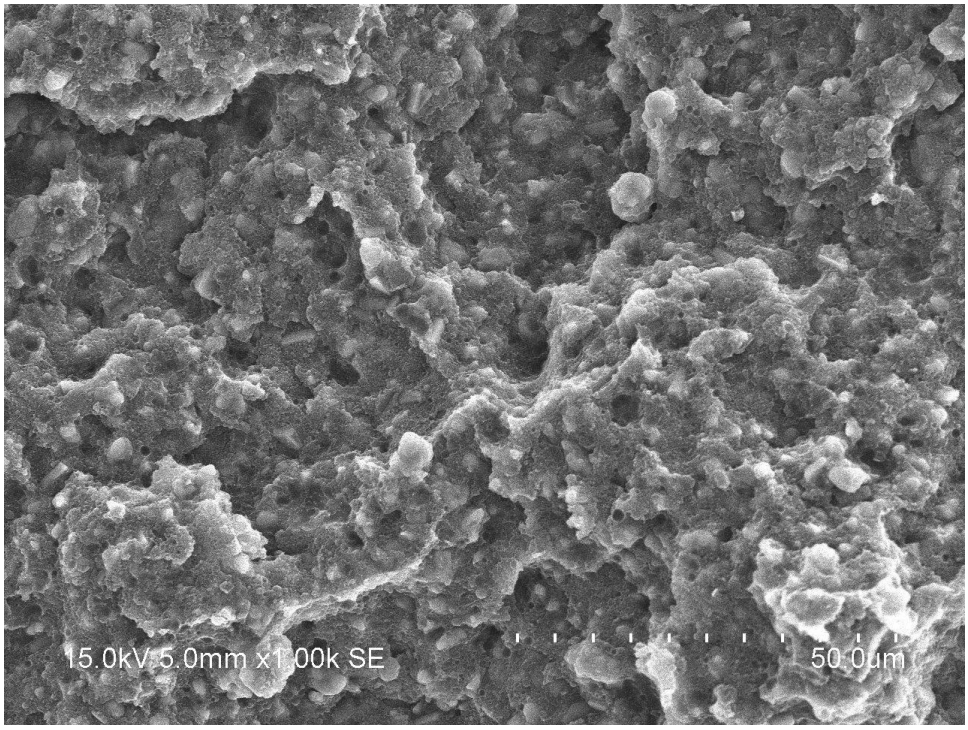

Figure 4.24: SEM micrographs of 150 kGy irradiated MOH-ABS composites with 20 phr zinc borate (ZB)

In general, by observing the surface of ATH-ABS composites and MOH-ABS composites had the similar morphologies of flakes. These flakes responsible to the low elongation at break of the composites.

4.4 Limiting Oxygen Index (LOI)

According to Figure 4.25, the addition of ZB to 10 phr caused the LOI value of all composites to increase. The addition of ZB could improve the flammability of the ATH-ABS composites. Mergen, et al. (2012) also observed the similar flammability changes with the increasing loading level of ZB. This flame retardants can function in both gas and condensed phases of the combustion process. When ZB is subjected to flame, ZB undergoes dehydration and dilutes the concentration of H radical and organic volatiles in the flame. After dehydration, the residual borate retained in the decomposed polymer will form a barrier which decelerates the

permeation of oxygen into the composites through surface. The more ZB added into the composites, there will be more barrier formed to slow down the permeation of volatile compounds and cause an increment in LOI. Formicola, et al. (2009) stated that the combination of ATH and ZB had the synergy effect on flammability behaviour the composites. Therefore, as the loading level of ZB is increased, the synergy effect between ATH and ZB fillers increases further and LOI is increased.

In addition, the irradiation dosages were observed to have effect on the LOI of ATH-ABS composites but the effect was minor. As shown in Figure 4.25, the higher the irradiation dosages subjected to the composites, the higher the LOI value of the composites. As studies carried by Bee, et al. (2013), the crosslinking network improved the flammability by two ways. The crosslinking network delayed dripping effect of the composites during burning. Moreover, the crosslinking network formed a barrier which can prevent the penetration of oxygen into the ABS matrix; thus slowing down the combustion rate of ATH-ABS composites.

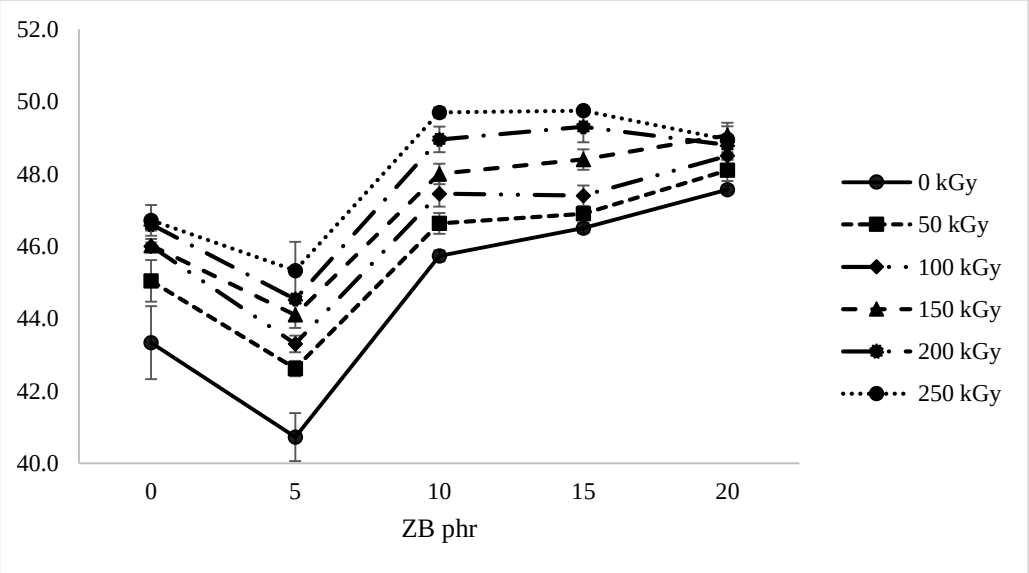

Figure 4.25: Limiting oxygen index of ATH-ABS composites filled with increasing of zinc borate (ZB) loading level under various electron beam irradiation dosages.

The LOI result of MOH-ABS composites was shown in Figure 4.26. When loading level of ZB increased from 0 to 10 phr, the LOI of all MOH-ABS composites gradually increased. The addition of ZB to 15 phr in the composites which subjected

to low irradiation dosages (0 kGy, 50 kGy, 100 kGy and 150 kGy) showed the continuous increment of LOI whereas the composites subjected with high irradiation dosages (200 kGy and 250 kGy) had decreased in flammability. Although it was expected the LOI value would increase with increasing ZB loading level, however all MOH-ABS composites had a decreasing LOI value as ZB loading level increased from 15 phr to 20 phr. In general, as the loading level of flame retardant fillers ZB added to the composites increase, the flame retardancy ability of the composites is improved and shows an increment in LOI result. This is because a slightly significant performance synergies between MOH and ZB to improve the composites flame retardancy. Chen and Shen (2005) also observed the similar increment in flammability when ZB mixed with MOH and concluded that ZB had further slowdown the rate of heat release and a strong char or residue will form within the composites. These barriers will block the volatile compounds to penetrate into the composites, thus slowing the burning process. In the end, the LOI result of MOH-ZB composites increases.

On the other hand, higher irradiation dosages also showed to have enhancement effect on the MOH-ABS composites. This is because high irradiation dosages inducing more free radicals to form larger crosslinking network within ABS matrix. Consequently, the large crosslinking network also have a more coverage as oxygen barrier and can prevent more oxygen for penetrating into the matrix; therefore improving the flammability of the MOH-ABS composites (Bee, et al., 2013).

By comparing the LOI value of ATH-ABS composites with MOH-ABS composites, the MOH-ABS composites had a higher flammability than ATH-ABS composites. This is because MOH has a higher endothermic dehydration than ATH; therefore this enables MOH to absorb more heat and have higher flammability; thus the LOI of the composites increases.

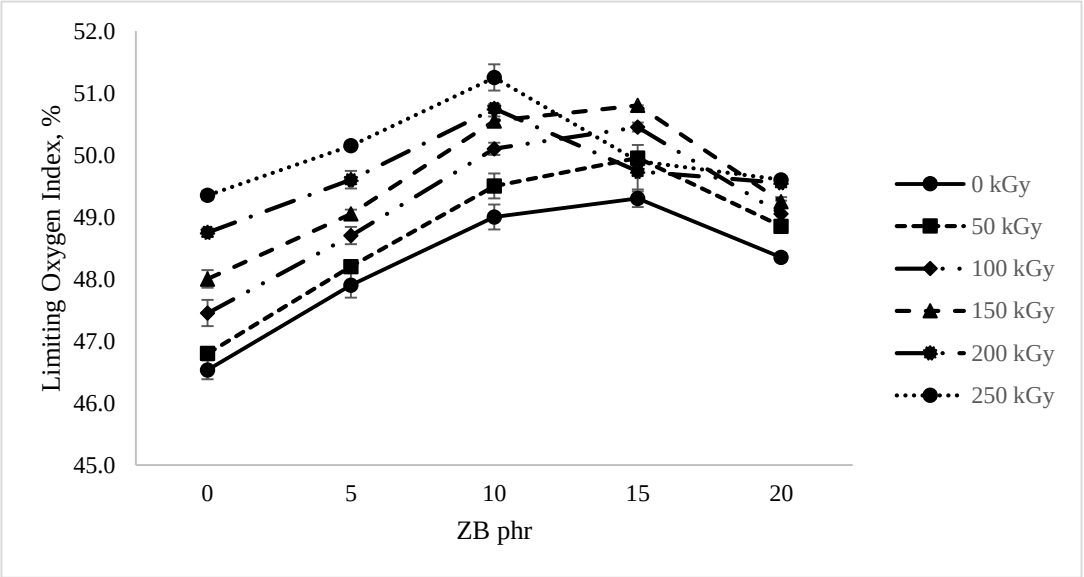

Figure 4.26: Limiting oxygen index of MOH-ABS composites filled with increasing of zinc borate (ZB) loading level under various electron beam irradiation dosages.

CHAPTER 5

CONCLUSION AND RECOMMENDATIONS

5.1 Conclusion

This study has investigated the flammability of ATH-ABS composites and MOH-ABS composites depended on loading level of ZB and irradiation dosage. However, the addition of loading level of ZB and irradiation dosage would also affect the mechanical properties of ATH-ABS composites and MOH-ABS composites. The irradiation dosage decreased the solubility of the composites.

The crosslinking effect of the ATH-ABS and MOH-ABS composites was not continuous. This is because irradiation dosages with more than 100 kGy could cause the degradation of butadiene which responsible for the rubbery properties of the composites and contributed to the destruction of crosslinking structure. \ Furthermore, the benzene rings of styrene inhibited the crosslinking effect. When the benzene rings were subjected to high irradiation dosages, it would breakdown and release plenty of linear polymeric free radicals. These free radicals would perform crosslinking and form the three-dimensional network within the matrix. Therefore, the crosslinking effect increased.

The changes in ZB loading level and irradiation dosages altered the mechanical properties of the composites. When the loading level of ZB in the ATH-ABS and MOH-ABS composites increased, its tensile strength also increased but elongation at break decreased. Besides that, the stiffness of the composites also improved because Young Modulus had increased when high ZB loading level was added. Furthermore,

the application of irradiation dosages on the ATH-ABS and MOH-ABS composites showed a slightly increment in the tensile strength of the composites. This was due to the high irradiation dosages induced more polymeric free radicals to form crosslinking network and then strengthened the tensile strength of the composites. However, the elongation at break was affected significantly when the composites were irradiated at high irradiation dosages. This was because the high irradiation dosages caused butadiene impact modifier to degrade and also breakdown the benzene ring of styrene. The degradation of butadiene impact modifier caused the composites to be more brittle and thus breakdown of benzene ring generates more linear polymeric free radicals which performed crosslinking to form three-dimension network. This network would decrease the mobility of the polymer chain within ABS matrix; making the composites to have a lower elongation at break. Moreover, the irradiation dosages had observed to have minor effect on the Young Modulus of the composites.

According to the surface morphologies, the un-irradiated ATH was not firmly bonded within ABS matrix but this interfacial adhesion between ATH and ABS could be improved when subjected to electron beam irradiation. Furthermore, when high loading level (20 phr) of ZB was added into ATH-ABS composites, the ZB fillers tended to form agglomerate which would affect the crosslinking effect and its mechanical properties. For un-irradiated MOH-ABS composites, the surface morphology showed MOH had a better interfacial adhesion with ABS than ATH fillers. However, when MOH-ABS composites were irradiated, the formation of small bubble voids would occur throughout the surface of the composites. The formation of small bubble voids could be prevented when 20 phr of ZB was added into the irradiated MOH-ABS composites.

Based on the result presented, it is clear that loading level of ZB and irradiation dosages could affect the flammability of ATH-ABS composites and MOH-ABS composites. The addition of ZB into both composites had induced the increase in LOI which represented the degree of flammability. When a higher loading level of ZB added into the composites, the composites flammability will be higher. On the other hand, the high irradiation dosages also induced numerous polymeric free radicals which will perform crosslinking process to form a three-dimensional network. These

three-dimensional network will aid in preventing the penetration of oxygen into ABS matrix.

5.2 Recommendation for Future Works

The ATH-ABS and MOH-ABS composites had a high loading level of ATH and MOH flame retardants fillers. It caused the ABS to lose its resistance impact and the samples was quite brittle. To retain the impact properties of ABS, try to use lower loading level of ATH and MOH fillers to blend with ABS. The loading level of ATH and MOH used in the blends should be lower than 40 phr.

The mechanical properties of ATH-ABS and MOH-ABS composites had been affected with the increasing irradiation dose. It had been observed that irradiation dosages over 100 kGy had significantly altered the properties of the composites. The high irradiation dosage degraded the butadiene which responsible to the rubbery properties of ABS. Further increase in irradiation dosage would breakdown the benzene ring to produce plenty of linear polymeric free radicals to perform crosslinking and formed three-dimensional network within the matrix. Therefore, in order to retain the original properties of ABS, irradiation dosages which lower than 100 kGy should be used to investigate the relationship between irradiation dosages with mechanical properties of the composites.

The processing temperature of 175 to 190˚C for barbender mixing was expected to be high as the dehydration process of ATH was around. Hence a lower processing temperature for barbender mixing should be used. The suggested processing temperature was probably in between of 150 to 175˚C.

REFERENCES

Alger, M., 1997. *Polymer Science Dictionary*. [e-book] London: Chapman & Hall. Available at: Google Books <http://books.google.com.my/books?id=OSAaRwBXGuEC&printsec=frontcover&dq=Polymer+Science+Dictionary&hl=en&sa=X&ei=sWneU7DxMpGJuATiwYLACg&redir_esc=y#v=onepage&q=Polymer%20Science%20Dictionary&f=false> [Accessed 3 August 2014].

Barati, A., Salbi, G., & Miri, T., 2012. Flame Retardant Effects of Nano-Clinoptilolite on Acrylonitrile-Butadiene-Styrene (ABS) Nano-Composite. *International Journal on Advanced Science Engineering Information Technology*, 2, 35-37.

Basfar, A., 2003. Effect of various combinations of flame-retardant fillers on flammability of radiation cross-linked poly(vinyl chloride) (PVC). *Polymer Degradation and Stability*, 82(2), pp. 333-340.

Bee, S. T., Hassan, A., Ratnam, C. T., Tee, T. T. and Lee, T. S., 2012. Effects of Montmorillonite on the Electron Beam Irradiated Alumina Trihydrate Added Polyethylene and Ethylene Vinyl Acetate Nanocomposite. *Polymer Compsites*, 33(11), pp. 1883-1892. doi:10.1002/pc.22328

Bee, S. T., Hassan, A., Ratnam, C. T., Tee, T. T. and Lee, T. S., 2013. Interactions of montmorillonite and electron beam irradiation in enhancing the properties of alumina trihydrate-added polyethylene and ethylene vinyl acetate blends. *Journal of Composite Materials*, 0(0), pp. 1-7.

Bhattacharya, A., Rawlins, J. W. and Ray, P., 2009. *Polymer Grafting and Crosslinking*. [e-book] Hoboken: John Wiley & Sons, Inc. Availabel at Google Books <http://books.google.com.my/books?id=n7ltMO8y95MC&printsec=frontcover&dq=Polymer+Grafting+and+Crosslinking&hl=en&sa=X&ei=MW3eU_amEYnJuASR1oE4&redir_esc=y#v=onepage&q=Polymer%20Grafting%20and%20Crosslinking&f=false> [Accessed 3 August 2014].

Borel, A., Ollé, A., Vergès, J. M. and Sala, R., 2014. Scanning Electron and Optical Light Microscopy: two complementary approaches for the understanding and interpretation of usewear and residues on stone tools. *Journal of Archaeological Science*, 48, pp. 46-59.

Carpentier, F., Bourbigot, S., Bras, M. L., & Delobel, R., 2000. Rheological investigations in fire retardancy: application to ethylene-vinyl-acetate copolymer-magnesium hydroxide/zinc borate formulations. *Polymer International*, 49, 1216-1221.

Chen, T & Shen, K., 2005. *Synergistic Benefits of Metal Hydroxides and Zinc Borate in Flame Retardant Wire and Cable Performance Compounds*. In: 54th International Wire & Cable Symposium Conference. USA, 13-16 November 2005. Providence: International Wire & Cable Symposium (IWCS) 2005. Available at: <http://www.hubermaterials.com/userfiles/files/PFDocs/Synergistic%20Benefits%20of%20Metal%20Hydroxides%20and%20Zinc%20Borate%20in%20Flame%20Retardant%20Wire%20and%20Cable%20Performance%20Compounds.pdf> [Accessed 3 August 2014].

Cleland, M. R., 2006. Industrial applications of electron accelerators. *Ion Beam Applications*, pp. 383-416.

Dolbey, R. ed., 1997. *Rapra Review Report*. [e-book] Shrewsbury: Rapra Technology Limited. Available at: Google Books <http://books.google.com.my/books?id=AcNSoQ9X7zoC&pg=PP2&dq=Rapra+Review+Report+Dolbey&hl=en&sa=X&ei=PXDeU4vOJtKhugS5o4GICw&redir_esc=y#v=onepage&q=Rapra%20Review%20Report%20Dolbey&f=false> [Accessed 3 August 2014].

Driscoll, S. B. ed., 1998. *The Basics of Testing Plastics: Mechanical Properties, Flame Exposure, and General Guidelines*. [e-book] West Conshohocken: American Society for Testing and Materials. Available at: Google Books <http://books.google.com.my/books?id=Bb0Ea4Q3dHoC&printsec=frontcover#v=onepage&q&f=false> [Accessed 3 August 2014].

Electron Microscopy of Mollicutes: Challenges and Opportunities. [pdf] Clemson: Clemson University. Avialable at: <https://www.google.com.my/search?q=Scanning+Electron+Microscopy+and+Transmission+Electron+Microscopy+of+Mollicutes%3A+Challenges+and+Opportunities&oq=Scanning+Electron+Microscopy+and+Transmission+Electron+Microscopy+of+Mollicutes%3A+Challenges+and+Opportunities&aqs=chrome..69i57.282470j0j7&sourceid=chrome&es_sm=122&ie=UTF-8> [Accessed 3 August 2014].

Fang, Y., Wang, Q., Guo, C., Song, Y. and Cooper, P. A., 2013. Effect of zinc borate and wood flour on thermal degradation and fire retardancy of polyvinyl chloride (PVC) composites. *Journal of Analytical and Applied Pyrolysi*, 100, pp. 957-962.

Formicola, C., De Fenzo, A., Zarrelli, M., Frache, A., Giodano, M. and Camino, G., 2009. Synergistic effects of zinc borate and aluminium trihydroxide on flammability behaviour of aerospace epoxy system. *Express Polymer Letters*, 3(6), pp. 376-384.

Fouassier, J. P., 1993. *Radiation Curing in Polymer Science and Technology: Fundamentals and Methods (Vol. 1)*. [e-book] Barking: Elsevier Science Publishers Ltd. Available at: Google Books <http://books.google.com.my/books?id=iqs0svYs8a8C&printsec=frontcover#v=onepage&q&f=false> [Accessed 3 August 2014].

Fried, J. R., 2009. *Polymer Science & Technology*. 2nd ed.. Westford: Pearson Education, Inc.

Harper, C. A. and Petrie, E. M., 2003. *Plastics Materials and Processes*. [e-book] New Jersey: John Wiley & Sons, Inc. Available at: Google Books <http://books.google.com.my/books?id=oe5YJmRmxQMC&printsec=frontcover&dq=Plastics+Materials+and+Processes.+Harper&hl=en&sa=X&ei=hXLeU4miCY6zuASF8IHgCg&redir_esc=y#v=onepage&q=Plastics%20Materials%20and%20Processes.%20Harper&f=false> [Accessed 3 August 2014].

Harwick Standard Distribution Corporation, 2008. Flame Retardants. [PDF] Ohio: Harwick Standard. Available at: <http://harwickstandard.com/technical/FlameRetardants.pdf> [Accessed 26 June 2011].

Horrocks, A. R. and Price, D., 2001. *Flame retardant materials*. [e-book] Cambridge: Woodhead Publishing Limited. Available at: Google Books <http://books.google.com.my/books?id=oe5YJmRmxQMC&printsec=frontcover&dq=Plastics+Materials+and+Processes.+Harper&hl=en&sa=X&ei=hXLeU4miCY6zuASF8IHgCg&redir_esc=y#v=onepage&q=Plastics%20Materials%20and%20Processes.%20Harper&f=false> [Accessed 3 August 2014].

Huber Engineered Materials. [No date]. *Alumina Trihydrate (ATH) & Magnesium Hydroxide (MDH)*. [pdf] Atlanta, USA: Huber Engineered Materials. Available at:<http://www.hubermaterials.com/userfiles/files/PFDocs/Huber%20Fire%20Retardant%20Additives%20(European%20Version).pdf> [Accessed 3 August 2014].

Katz, H. S. and Milewski, J. V. ed., 1987. *Handbook of Fillers For Plastics*. [e-book] New York: Van Nostrand Reinhold. Available at: Google Books <http://books.google.com.my/books?id=zKMiAEVWgUIC&printsec=frontcover&dq=Handbook+Of+Fillers+For+Plastics&hl=en&sa=X&ei=xXXeU5SXLI-1uAShq4CQBw&ved=0CBwQ6AEwAA#v=onepage&q=Handbook%20Of%20Fillers%20For%20Plastics&f=false> [Accessed 3 August 2014].

Landi, T. R. L., 2003. *Radiation Effect Study By Electron Beam Ionizing on Acrylonitrile Butadiene Styrene Terpolymer*. [online] Available at: < http://pelicano.ipen.br/PosG30/TextoCompleto/Tania%20Regina%20de%20Lourenco%20Landi_M.pdf> [Accessed 28 March 2015].

Liu, H., Fang, Z., Peng, M., Shen, L. and Wang, Y., 2009. *The effects of irradiation cross-linking on the thermal degradation and flame-retardant properties of the*

HDPE/EVA/magnesium hydroxide composites, 78, pp. 922-926. doi:10.1016/j.radphyschem.2009.06.013

Liu, S. P., 2014. Flame retardant and mechanical properties of polyethylene/magnesium hydroxide/montmorillonite nanocomposites. *Journal of Industrial and Engineering Chemistry*, 20(4), pp. 2401-2408.

Machi, S., 1996. New Trends of Radiation Processing Applications. *Radiat. Phys. Chem.*, 47(3), pp. 333-336.

Makuuchi, K. and Cheng, S., 2012. *Radiation Processing of Polymer Materials and its Industrial Applications*. [e-book] Hoboken: John Wiley & Sons, Inc. Available at: Google Books <http://books.google.com.my/books?id=rmXWy9pe8ZYC&printsec=frontcover&dq=Radiation+Processing+of+Polymer+Materials+and+its+Industrial+Applications&hl=en&sa=X&ei=NHbeU__uA8S_uASd8oD4DQ&ved=0CBwQ6AEwAA#v=onepage&q=Radiation%20Processing%20of%20Polymer%20Materials%20and%20its%20Industrial%20Applications&f=false> [Accessed 3 August 2014].

Mergen, A., İpek, Y., Bölek, H. and Ökuüz, 2012. Production of nano zinc borate (4ZnO·B2O3·H2O) and its effect on PVC. *Journal of the European Ceramic Society*, 32, pp. 2001-2005.

Natwig, G. S., 1984. Track and erosion resistance electrical insulation comprising zinc borate and ethylene polymer. US Patent 4426549 A.

Nelson, M., 2002. *Combustion of Polymers: Oxygen-Index Methods*. [online] Available at: < http://www.uow.edu.au/~mnelson/review.dir/oxygen.html> [Accessed 3 August 2014].

New ATH developments drive flame retardant cable compounding, 2002. *Plastics Additives & Compounding*, 4(12), pp. 22-29.

Pentimalli, M., Capitani, D., Ferrandi, A., Ferri, D., Ragni, P. and Segre, A. L., 1996. Gamma irradiation of food packaging materials: an NMR study. *Polymer*, 41(8), pp. 2871-2881.

Polymer Crosslinking, [No date]. [online] Available at: <http://www.rsccaerodefense.com/polymer-cross-linking.php#.U9uW7PmSzIs> [Accessed 3 August 2014].

Radiation vs. Chemical Crosslinking for Polymer Parts, 2005. [pdf]. Available at: <http://www.sterigenics.com/services/advanced_applications/radiation_processing/Radiation_vs._Chemical_Crosslinking_for_Polymer_Parts.pdf. [Accessed 3 August 2014].

Sabet, M., Hassan, A. and Ratnam, C. T., 2012. Electron beam irradiation of low density polyethylene/ethylene vinyl acetate filled with metal hydroxides for wire and cable applications. *Polymer Degradation and Stability*, 97(8), pp. 1432-1437.

Sain, M., Park, S.H., Suhara, F. and Law, S., 2004. Flame retardant and mechanical properties of natural fibre-PP composites containing magnesium hydroxide. *Polymer Degradation and Stability*, 83(2), pp. 363-367.

Sanchez-Olivares, G., Sanchez-Solis, A., Calderas, F., Medina-Torres, L., Herrera-Valencia, E.E., Castro-Aranda, J.I., Manero, O., Di Blasio, A. and Alongi, J., 2013. Flame retardant high density polyethylene optimized by on-line ultrasound extrusion. *Polymer Degradation and Stability*, 98(11), pp. 2153-2160.

Smits, V. and Materne, T., 2005. *The Eighth International Conference on Thermoplastic Elastomers*. In: 8th International Conference on Thermoplastic Elastomers. Germany, 14-15 September 2005. [e-book] Shrewsbury: Rapra Technology Limited. Available at: <http://books.google.com.my/books?id=DxLGxneuP0gC&printsec=frontcover#v=onepage&q&f=false> [Accessed 3 August 2014].

Stadtländer, C. T. K.-H., 2007. Scanning Electron Microscopy and Transmission. *Modern Research and Educational Topics in Microscopy*, pp. 122-131.

Suzanne, M., Delichatsios, M. A. and Zhang, J. P., 2013. Flame extinction properties of solids obtained from limiting oxygen index tests. *Combustion and Flame*, 161(1), pp. 288-294.

Tendero, P. M. R., Jiménez, A., Greco, A. and Maffezzoli, A., 2005. *Crosslinking of PVC Plastisols by Reactive Processing*. In G. E. Zaikov, Y. B. Monakov & A. Jiménez, eds. Trends in Molecular and High Molecular Science. [e-book] New York: Nova Science Publishers, Inc. pp. 123-141. Available at: Google Books <http://books.google.com.my/books?id=3sqvDU4NMrMC&printsec=frontcover&dq=Trends+in+Molecular+and+High+Molecular+Science&hl=en&sa=X&ei=o3reU6TaI5PGuATezIGABQ&ved=0CBwQ6AEwAA#v=onepage&q=Trends%20in%20Molecular%20and%20High%20Molecular%20Science&f=false> [Accessed 3 August 2014].

Tillet, G., Boutevin, B. and Ameduri, B., 2011. Chemical reactions of polymer crosslinking and post-crosslinking at room and medium temperature. *Progress in Polymer Science*, 36(2), pp. 191-217.

Walter, M. D. and Wajer, M. T., [No date]. *Overview of Flame Retardants Including Magnesium Hydroxide*. [pdf] Baltimore: Martin Marietta Magnesia Specialties, LLC. Available at: <http://www.magnesiaspecialties.com/pdf/flame-retardants.pdf> [Accessed 3 August 2014].

West, A. R. 1990. *Solid State Chemistry and Its Applications*. [e-book] Hoboken: John Wiley & Sons, Inc. Available at: Google Books <http://books.google.com.my/books?id=-EKCm5UQaqEC&printsec=frontcover#v=onepage&q&f=false> [Accessed 3 August 2014].

Whealan, T., 1994. *Polymer Technology Dictionary*. [e-book] London: Chapman & Hall. Available at: Google Books <http://books.google.com.my/books?id=7Qq_vknrP4kC&printsec=frontcover#v=onepage&q&f=false> [Accessed 3 August 2014].

Xanthos, M. ed., 2010. *Functional Fillers for Plastics: Second, updated and enlarged edition*. [e-book] Weinheim: WILEY-VCH Verlag GmbH & Co. KGaA. Available at: Google Books <http://books.google.com.my/books?id=szxZlU68kEYC&pg=PP1&dq=Functional+Fillers+for+Plastics:+Second,+updated+and+enlarged+edition&hl=en&sa=X&ei=b33eU4KaD9COuAT1lYGABg&ved=0CCUQ6AEwAA#v=onepage&q=Functional%20Fillers%20for%20Plastics%3A%20Second%2C%20updated%20and%20enlarged%20edition&f=false> [Accessed 3 August 2014].

Yidiz, B., Seydibeyoğlu, M. O. and Güner, F. S., 2009. Polyurethane-zinc borate composites with high oxidative stability and flame retardancy. *Polymer Degradation and* Stability, 94(7), pp. 1072-1075.

Zhang, X., Guo, F., Chen, J., Wang, G. and Liu, H., 2005. Investigation of interfacial modification for flame retardant ethylene vinyl acetate copolymer/alumina trihydrate nanocomposites. *Polymer Degradation and Stability*, 87(3), pp. 411